JAERI-M
88-164

NEANDC(J)-131/U
INDC(JPN)-117/L

REVISION AND STATUS OF THE NEUTRON NUCLEAR DATA OF ^{6}Li AND ^{7}Li

August 1988

Satoshi CHIBA and Keiichi SHIBATA

日本原子力研究所
Japan Atomic Energy Research Institute

JAERI-Mレポートは，日本原子力研究所が不定期に公刊している研究報告書です。
入手の問合わせは，日本原子力研究所技術情報部情報資料課（〒319-11茨城県那珂郡東海村）あて，お申しこしください。なお，このほかに財団法人原子力弘済会資料センター（〒319-11 茨城県那珂郡東海村日本原子力研究所内）で複写による実費頒布をおこなっております。

JAERI-M reports are issued irregularly.
Inquiries about availability of the reports should be addressed to Information Division Department of Technical Information, Japan Atomic Energy Research Institute, Tokai-mura, Naka-gun, Ibaraki-ken 319-11, Japan.

編集兼発行　日本原子力研究所
印　　刷　いばらき印刷㈱

JAERI-M 88-164

Revision and Status of the Neutron Nuclear Data of ^{6}Li and ^{7}Li

Satoshi CHIBA and Keiichi SHIBATA

Department of Physics
Tokai Research Establishment
Japan Atomic Energy Research Institute
Tokai-mura, Naka-gun, Ibaraki-ken

(Received July 29, 1988)

The neutron nuclear data of ^{6}Li and ^{7}Li stored in JENDL-3PR1 have been partly revised for JENDL-3 by taking account of the experimental data measured after their evaluations. The revision was mainly based on the double-differential neutron emission cross section data measured in Japan. The $^{7}Li(n, n't)\alpha$ reaction cross section was slightly enhanced around 14 MeV on the basis of recently measured data using the tritium counting method. The spectra of the continuum secondary neutrons produced by the $^{6}Li(n, n'd)\alpha$ and $^{7}Li(n, n't)\alpha$ reactions were calculated by the three-body phase-space model with the Coulomb interaction between the two charged particles in the final states. In the evaluated files, they were described by about 30 pseudo levels with a 0.5 MeV interval. The secondary neutron spectra from the $^{6}Li(n, 2n)$ and $^{7}Li(n, 2n)$ reactions were given by the conventional evaporation mode. Two higher resonant states, which had not been contained in the JENDL-3PR1 evaluation, were included in the present evaluation for each nuclide. A coupled-channel chalculation was performed to interpolate and extrapolate the elastic and some inelastic scattering cross sections. The present revision was restricted to the neutron emitting reactions. In this report, method of the revision and status of the produced data files are described.

Keywords: Revision, Neutron Nuclear Data, Lithium-6, Lithium-7, Phase-space Model with Coulomb Interaction, Pseudo Levels, (n, 2n) Reaction, Evaporation Model, Coupled-channel Calculation, Cross Section, JENDL-3

JAERI－M 88－164

^{6}Liと^{7}Liの中性子核データの改訂と現状

日本原子力研究所東海研究所物理部
千葉　敏・柴田　恵一

（1988年7月29日受理）

最近の実験データを考慮して，JENDL－3PR1に格納されている^{6}Liと^{7}Liの中性子核データをJENDL－3のために部分的に改訂した。この改訂は主として，日本で測定された中性子の二重微分断面積を考慮して行った。また，^{7}Li(n，n't)α反応の断面積も，最近行われたトリチウム計測の方法による測定データを考慮した結果，14MeV領域でより大きな値であることがわかった。^{6}Li(n，n'd)α反応と^{7}Li(n，n't)α反応から放出される連続的な形状を持つ二次中性子のスペクトルについては，終状態での二つの荷電粒子の間に働くクーロン相互作用を考慮した三体の位相空間分布により計算した。評価済みデータとしては，それらを0.5MeV間隔で設けた約30本の疑似準位（pseudo level）によって記述した。また，^{6}Li(n，2n)反応と^{7}Li(n，2n)反応から放出される二次中性子のスペクトルは蒸発模型で与えた。さらに，各原子核に対して，JENDL－3PR1で考慮されていなかった高励起状態をそれぞれ2本ずつ新たに加えた。弾性散乱と非弾性散乱断面積をデータの存在しない領域に内挿，及び外挿するために，チャンネル結合法による計算も行った。今回の改訂は中性子を放出する反応に限ったものであるが，本報告では，その改訂の手法と完成したデータファイルの現状について記述する。

東海研究所：〒319－11 茨城県那珂郡東海村白方字白根2－4

Contents

目　　次

1. Introduction

The preliminary version of Japanese Evaluated Nuclear Data Library 3 (JENDL-3PR1)[1] was prepared in December 1983 to respond to the strong requests from the analysts of the Japan-US cooperative experiment using the JAERI Fusion Neutronics Source (FNS) and of the University jointed programs on fusion experiments using the intense 14-MeV neutron source at Osaka University (OKTAVIAN). The JENDL-3PR1 consists of the data for eight nuclides, ^{6}Li, ^{7}Li, ^{9}Be, ^{12}C, ^{16}O, Cr, Fe and Ni. These nuclear data are essential for the design of neutronic properties of fusion reactors. They were intended to resolve the drawbacks in JENDL-2[2] when applied to fusion neutronics calculations. The main purpose was to give evaluated nuclear data files that can reproduce the experimental data on the double-differential neutron emission cross sections (DDX), measurements of which were just started very intensively in Japan at that time.

The problems for the structural materials, Cr, Fe and Ni, were mainly due to lack of the direct and pre-equilibrium components of the inelastic neutron scattering in the JENDL-2 evaluation[3]. Therefore the spectra of the secondary neutrons produced by the inelastic scattering and some reactions were too soft compared with the measured DDX data. In JENDL-3PR1, the contributions of these processes were calculated and added to the JENDL-2 data which were evaluated on the basis of the statistical model. The JENDL-3PR1 data reproduce the measured DDX data very well as a whole.

On the contrary, the continuum neutron spectra produced by interaction of neutrons with the light nuclides are produced by the few-body break-up reactions. Mechanisms of these reactions are not understood well at present, and the statistical and pre-equilibrium models are no longer good approximations for these nuclides. Hence they can not be appropriately applied to the light-nuclide evaluations. There seem to be at present no "a-priori" way to calculate the continuum neutron spectrum emitted from light nuclides with good accuracy.

In JENDL-3PR1, the neutron nuclear data of lithium were evaluated by Shibata[4,5]. The continuum neutron spectra produced by the ^{6}Li(n,n'α) and ^{7}Li(n,n't)α reactions were calculated by the three-body phase-space model, as well as the ^{6,7}Li(n,2n) reactions. Two excited levels were considered for each nuclide.

After the evaluation of the neutron nuclear data of ^{6}Li and ^{7}Li for

JENDL-3PR1, the DDX data were measured at Osaka University around 14 MeV using a natural lithium sample[6], and at Tohoku University at 4.2, 5.4 and 14.2 MeV for ^{6}Li and at 5.4, 6.0 and 14.2 MeV for ^{7}Li using isotopically enriched samples[7]. They compared their data with the prediction of JENDL-3PR1 and concluded that there were still some problems in JENDL-3PR1. The main features of these problems were common to both groups and are summarized as follows;

1) Some higher resonant states, which were not included in the JENDL-3PR1 evaluation, should be taken into account as discrete levels.
2) The energy spectra of the continuum neutrons emitted from the ^{6}Li(n,n'd)α and ^{7}Li(n,n't)α reactions, as well as the ^{6,7}Li(n,2n) reactions, are not appropriately given in JENDL-3PR1.
3) The ^{6}Li(n,2n) reaction cross section is overestimated by about 20% in the 14-MeV region.
4) The angular distributions of inelastically scattered neutrons from ^{7}Li should be anisotropic in the center-of-mass system.

These suggestions are considered to be highly reliable, because these problems were also pointed out from the analyses of some integral expeirments by Hashikura[8] and Sugiyama[9].

Besides the problems mentioned above, the cross section of the ^{7}Li(n,n't)α reaction stored in JENDL-3PR1 was pointed out to be too small compared with the high accuracy tritium counting experiments[10] preformed recently around 14 MeV. Furthermore, according to the recent data, the ^{7}Li(n,n')^{7}Li (Q=-4.63 MeV) reaction cross section might be overstimated in the energy range of 7 to 13 MeV. Considering these problems, we decided that the neutron nuclear data for ^{6}Li and ^{7}Li stored in JENDL-3PR1 should be revised partly.

This report describes the method of the revision and full results of the produced data files. In the following sections, the method of revising the neutron nuclear data of ^{6}Li and ^{7}Li stored in JENDL-3PR1 is described. Those data not revised in the present evaluation are also presented to be complete and for users' convenience sake. All the data span the energy range from 10^{-5} eV or the threshold to 20 MeV. The status of the presently revised quantities is listed in Table 1.

2. Revision and Status of the Neutron Nuclear Data for ^{6}Li

The total, elastic and inelastic scattering, radiative capture, photon-production, (n,2n), (n,p) and (n,α) reaction cross sections and the angular and energy distributions of secondary neutrons were evaluated in JENDL-3PR1[4]. Among them, the elastic and inelastic scattering and (n,2n) reaction cross sections and angular and energy distributions of secondary neutrons have been revised in the present evaluation.

2.1 Total Cross Section

The total cross section was not changed from the JENDL-3PR1 evaluation.

In JENDL-3PR1, the total cross section was calculated by the R-matrix theory below 1 MeV, using the code RESCAL[11]. Tow channels, the elastic scattering and (n,α) reaction, were taken into consideration. One negative and three positive resonances were included. With regard to the $P_{5/2}$ resonance at 250 keV, the following experimental data were considered for the fitting:

total cross section	Smith et al.[12]
elastic scattering cross section	Knitter et al.[13]
(n,α) reaction cross section	Macklin et al.[14]

The R-matrix parameters are listed in Table 2. The total cross section was calculated to be the sum of the elastic scattering cross section, the (n,α) reaction and the (n,γ) reaction cross sections, because the radiative capture cross section was not included in the R-matrix calculation.

Above 1 MeV, the total cross section was evaluated by fitting the spline function to the experimental data of Knitter et al.[13], Lamaze et al.[15], and Guenther et al.[16] using the Neutron Data Evaluation System (NDES)[21].

The results are shown in Figs. 1-3. The solid line labeled as SHIBATA is the data adopted in JENDL-3PR1 and it was also adopted in the present evaluation without any change.

2.2 Elastic Scattering Cross Section

The elastic scattering cross section of ^{6}Li was evaluated as follows:

below 1 MeV it was calculated by the R-matrix theory, i.e., no change from JENDL-3PR1. Above 1 MeV, it was given by subtracting the reaction cross section from the total cross section. The presently evaluated elastic scattering cross section was slightly changed from JENDL-3PR1 data due to a change in the (n,2n) reaction cross section described below. The result is shown in Figs. 4 and 5.

Angular distribution of the elastic scattering was not also changed from JENDL-3PR1 below 14 MeV. It was calculated by the R-matrix theory below 500 keV. Between 500 keV and 14 MeV, the Legendre coefficients were obtained from the experimental data of Knitter et al. (500 keV ∿ 3 MeV)[13], Knox et al. (4 MeV ∿ 7.5 MeV)[30] and Hogue et al. (7.5 MeV ∿ 14 MeV)[29].

Above 14 MeV, the elastic scattering angular distribution for ^{6}Li was newly calculated by the coupled-channel theory assuming the symmetric rotational mode. The computer code ECIS79[34] was used in the calculations. The coupling scheme was taken to be 1+(G.S.) - 3+(2.185) - 2+(4.31) - 1+(5.7) (K=1 band). The optical potential and deformation parameters were taken from ref.35. These parameters were determined by fitting the experimental elastic and inelastic scattering data of Hogue et al.[29] between 9 and 14 MeV. Although applicability of the model to these light nuclei as lithium and validity of the parameters used will still be an open question, there seems to be no other way to calculate the angular distribution of elastic and inelastic scattering appropriately. The similar approach has been also made by Hansen[36] in the analysis of the ^{9}Be(n,n) reaction and by Koori et al.[37] in the ^{7}Li(p,p') reaction.

The angular distributions of elastically scattered neutrons from ^{6}Li are shown in Fig. 6. The agreement between the present evaluation and experimental data is generally very good as seen in the figure.

2.3 Inelastic Scattering Cross Section

2.3.1 The First Level (2.185 MeV)

The cross section to this level was not, except the angular distribution above 14 MeV, changed from JENDL-3PR1.

In JENDL-3PR1, the cross section to this level was evaluated with the eye-guide method by using NDES. The experimental data of Hogue et al. (7 MeV, 14 MeV)[29], Guenther et al. (3.5 MeV, 4.0 MeV)[16], Lisowski et al. (5.96 MeV, 9.83 MeV)[31], Fortsch et al. (7.75 MeV)[32] and Drake

(14 MeV)[41] were used. The result is shown in Fig. 7.

The angular distribution was estimated from the experimental data of Hogue et al.[29] and Hopkins et al.[27] below 14 MeV. Above 14 MeV, it was calculated by the coupled-channel theory described above. The angular distribution is shown in Fig. 8.

2.3.2 The Second Level (3.562 MeV)

The cross section and angular distribution for this level were not changed from JENDL-3PR1 evaluation. Note that this level decays by emitting γ-ray to the ground state and hence does not contribute to the $^{6}Li(n,n'd)\alpha$ reaction.

In JENDL-3PR1, the data of Presser et al. (4.1 MeV ∿ 7.0 MeV)[39] and Bestonsnyj et al. (14 MeV)[40] were adopted and the evaluation was made by fitting the spline function to these data with NDES. The result is plotted in Fig. 9 with experimental data.

The angular distribution was assumed to be isotropic in the center-of-mass system.

2.3.3 The Third Level (4.31 MeV)

This level was newly considered in the present evaluation. This level and the fourth level (5.7 MeV) were added to JENDL-3PR1 because the JENDL-3PR1 data did not reproduce the DDX experiments measured at En=14.2 MeV.

No excitation function and angular distribution were reported for this level. Therefore the cross section and angular distribution were calculated by the coupled-channel method described above. The calculated excitation function was normalized to the experimental data[7] at 14.2 MeV, although the numerical data on this peak were not published because of large uncertainties in yield estimation.

2.3.4 The Fourth Level (5.7 MeV)

This level was newly considered in the present evaluation. The reason has been already described above.

The cross section and angular distribution were calculated by the coupled-channel theory. The calculated excitation function was normalized to the experimental data at 14.2 MeV[7], although the experimental data have large errors and hence were not published.

2.3.5 Continuum Inelastic Scattering

The inelastic scattering cross section to the cotinuum state (break-up channel) was calculated to be the difference between the evaluated total $^{6}Li(n,n'd)\alpha$ reaction cross section and a sum of the discrete inelastic scattering cross sections except the second level which decays by the γ-ray transition. The total $^{6}Li(n,n'd)\alpha$ reaction cross section was evaluated based on the measurement of Rosen and Stewart[42]. The evaluated total Li(n,n'd) reaction cross section is plotted in Fig. 10 with the experimental data.

The angular and energy distributions for these neutrons were evaluated by the method that will be described in Sect. 2.9.

2.4 The $^{6}Li(n,2n)$ Reaction

There are three experimental data for this reaction. Two were obtained by the coincident counting method[43,44] and one by unfolding the measured secondary neutron spectrum assuming a simple functional form[7].

In the JENDL-3PR1 evaluation, these data except ref.7 were considered but the evaluated results were slightly modified so that the elastic scattering cross section reproduce the experimental data. This procedure resulted in the overestimation of the $^{6}Li(n,2n)$ reaction cross section as pointed out from the DDX measurement. In the present evaluation, therefore, these data[7,43,44] were directly adopted without any modification. The result is shown in Fig. 11.

The angular distributions of the secondary neutrons emitted from this reaction were replaced by the experimental data[7]. They are given in the laboratory system.

With regard to the energy distribution of the secondary neutrons for this reaction, the conventional evaporation model was assumed as described in ref.7. The evaporation temperature (θ) given in the reference was adopted at 14.2 MeV. This temperature was extraporated to lower and higher energy region assuming a relation which is deduced from the Fermi gas model;

$$\theta = (E/T)^{1/2}$$

where T is a constant.

2.5 The $^{6}Li(n,p)$ Reaction

The (n,p) reaction cross section was not changed from JENDL-3PR1. The evaluation curve follows the experimental data[45-49], as shown in Fig. 12.

2.6 The $^{6}Li(n,t)\alpha$ Reaction

This cross section was not revised. In JENDL-3PR1, it was calculated by the R-martrix theory below 1 MeV. The calculated thermal value of 940.33 barns is in good agreement with the value of 940 ± 4 barns recommended by Mughabghab et al.[50] The peak value of the $P_{5/2}$ resonance was calculated to be 3.364 barns at 230 keV.

Above 1 MeV, the experimental data of Bartle[51] and of Bartle et al.[52] were adopted and evaluation curve was determined by a least-squares fit to them. The $^{6}Li(n,t)\alpha$ reaction cross section is shown in Figs. 13-15.

2.7 The Radiative Capture Reaction

This cross section was not revised in the present evaluation. From 10^{-5} eV to 100 keV, the cross section was extrapolated as 1/v, normalizing the scale at the thermal energy to the recommendation of Mughabghab et al.[50], i.e., 38.5 mb. Above 100 keV, the inverse reaction data of Ferdinande et al.[59] were added by using the principle of the detailed balance. The result is shown in Fig. 16.

2.8 Photon Production Cross Section

The Photon Production data stored in JENDL-3PR1 have not been changed in the present evaluation. Because the threshold for the particle break-up is very low (Ex = 1.473 MeV), all the excited resonant states except the second level decay by particle emission prior to γ-ray transition. Hence we need only the photon production data for the second level and radiative capture channels.

2.8.1 The $^{6}Li(n,n_2\gamma)$ Reaction

The second state of ^{6}Li decays by emitting γ-rays into the ground

state with a probability of 100%. Thus the multiplicity for this γ-ray is 1.0. The angular distribution of this γ-ray is known to be isotropic.

2.8.2 The $^{6}Li(n,\gamma)$ Reaction

In JENDL-3PR1, the γ-ray multiplicities were deduced from the data of Jurney[60] as follows:

Transition		Multiplicity
cap.	→ g.s.	0.61
cap.	→ 0.47761 MeV	0.39
0.4776 MeV	→ g.s.	0.39

The augular distributions of the γ-rays were assumed to be isotropic.

2.9 The Angular and Energy Distribution of the Continuum Neutrons

In this section, a method is presented of obtaining the angular and energy distribution of the continuum neutrons emitted from the $^{6}Li(n,n'd)\alpha$ reaction.

In general, the double-differential cross section of producing particle 1 of an energy E in the direction $\Omega(\theta,\phi)$ is proportional to the product of the available phase-space volume and the reaction T-matrix element as follows:

$$d^2\sigma/(dEd\Omega) = 2\pi/v \cdot \rho(E,\theta) \cdot \int |T|^2 \, \Omega_{23} \qquad (1)$$

where v is the relative velocity between the projectile and targer, $\rho(E,\theta)$ the phase space factor, T the transition matrix and Ω_{23} the direction of the relative momentum between remaining two particles (2=d and 3=α, for example) in the final state. T contains all the physical information on the reaction mechanism. Here we assume the process represented generally by the following diagram is dominant.

$$\begin{array}{l} \overset{V}{p + T \rightarrow 1 +} \overset{U}{(2 + 3)} \\ \qquad\qquad\quad (2 + 3) \rightarrow 2 + 3 \end{array}$$

where p denotes the projectile (neutron), T the targer (^{6}Li), 1, 2 and 3 the three particles in the final state (put 1 = n, 2 = d and 3 = α here), V the potential that induces the first step reaction, U the potential between the two particles interacting in the final state. In this case the T-matrix can be written as[61]

$$T_{b\leftarrow a} = \int d^3q' \ \langle \psi_b^- \ | \chi(q') \rangle \ \langle \chi(q') | V \Psi_a^+ \rangle \tag{2}$$

where a and b denote the initial and final state, respectively, Ψ_a^+ and ψ_b^- the scattering state wave function in the initial and final states, respectively, and $\chi(q')$ a complete set of plane wave states. The producing term, $\langle \chi(q') | V \Psi_a^+ \rangle$, will not be dependent strongly on the relative momentum q between particle 2 and 3. Hence in the range of maximum contribution to the integral (where the final-state amplitude is maximum), the above equation can be approximated as

$$\begin{aligned} T_{b\leftarrow a} &\fallingdotseq \langle \chi_b | V \Psi_a^+ \rangle \int d^3q' \ \langle \psi_b^-(q) | \chi(q') \rangle \\ &= \langle \chi_b | V \Psi_a^+ \rangle \ \psi_{23}^{-*}(q, r_{23}=0) \end{aligned} \tag{3}$$

where $\psi_{23}(q, r_{23}=0)$ is the wave function for the relative motion of particle 2 and 3 at the origin and is called to be the factored wave function. Using this expression for the T-matrix, the energy and angular distribution of particle 1 (in this case, neutron) is written as

$$\begin{aligned} d^2\sigma/(dEd\Omega) &\sim \rho(E,\theta) \int |T|^2 \cdot d\Omega_{23} \\ &= \rho(E,\theta) \int |T^0|^2 \cdot |\psi_{23}^{-*}(q,0)|^2 \cdot d\Omega_{23} \\ &= A \cdot |\psi_{23}^{-*}(q,0)|^2 \cdot \rho(E,\theta) \end{aligned} \tag{4}$$

where A is an arbitrary constant factor which is independent of the secondary neutron energy and angle. The factor $|\psi_{23}^{-*}(q,0)|^2$ is interpreted as the density of the state of system 2 + 3. Because the resonant components that can be seen in the scattering cross section of d + α were already considered as the discretely excited atates in ^{6}Li, here we are concerned only with the non-resonant contribution. Therefore taking the pure Coulomb interaction as the potential U, the relative wave function between particles 2 and 3, $\psi_{23}^{-*}(q,0)$, reduces to a simple Coulomb wave function. Then the above equation becomes finally as follows

$$d^2\sigma/(dEd\Omega) = A\cdot 2\pi\eta/[\exp(2\pi\eta) - 1]\cdot\rho(E,\theta) \quad (5)$$

where $\eta = 2\pi Z_2 Z_3 e^2/(hv)$ is the Coulomb parameter for the particle 2 and 3 system, Z_2 and Z_3 are the charges of particle 2 and 3, respectively and h the Planck's constant. Though to take the pure Coulomb potential as the potential U is not, strictly speaking, allowed in this theory, we took this as the form representing the energy and angular distribution of the secondary continuum neutrons emitted from the ^{6}Li(n,n'd)α reaction in the present evaluation. This expression was found to reproduce the secondary neutron spectra produced by the ^{6}Li(n,n'd)α and ^{7}Li(n,n't)α reactions at low incident energies better than the phase-space model adopted in JENDL-3PR1. In the low incident neutron energy, only a few discrete levels are energetically open and it was easy to check the validity of the model that describes the continuum neutron spectra. This model was firstly suggested by Holland et al.[62] in the analysis of the neutron spectra measured in their experiment on the ^{6}Li(d,n^{3}He)α reaction.

The phase-space factor $\rho(E,\theta)$ is expressed very simply in the center-of-mass system as;

$$\rho(E,\theta) = C\cdot[E\cdot(E_{max} - E)]^{1/2}, \quad (0 < E < E_{max}) \quad (6)$$

ware E denotes the kinetic energy of the secondary neutrons relative to the center-of-mass of d+α system, E_{max} its kinematically allowed maximum energy and C a normalization constant. In this expression, it is assumed that the angular distribution of the secondary neutrons is isotropic in the center-of-mass system. Using the incident neutron energy (Eo) in the center-of-mass system, the reaction Q-value (Q) and the excitation energy (Ex) of the residual nucleus, the above relation is rewritten as follows;

$$\rho(E,\theta) = \rho'(Ex) = C\cdot[(Eo - Ex)\cdot(Q + Ex)]^{1/2}, \quad (-Q < Ex < Eo) \quad (7)$$

According to eqs.(5) and (7), the spectrum of secondary neutrons emitted from the ^{6}Li(n,n'd)α reaction was converted to the excitation energy spectrum in the ^{6}Li system.

In the present evaluation, pseudo levels were set in energy 0.5 MeV excitation energy interval. Thirty two pseudo levels were necessary

to cover the energy range from threshold to 20 MeV. The cross section for each level was calculated according to the excitation energy distribution given by eqs.(5) and (7). With this method, the continuum neutron spectrum produced by the ^{6}Li(n,n'd)α reaction was given by the sum of the inelastic scattering to these levels.

At the incident neutron energy of E_{lab}, the cross section for the i-th pseudo level, with the excitation energy E_i, can be calculated as follows if Eo ≧ E_i (otherwise it cannot be excited);

$$\sigma_i(E_{lab}) = \frac{\sigma_c(E_{lab}) \cdot \int_{\max(E_i-0.25\mathrm{MeV},-Q)}^{\mathrm{Eupper}} \Phi(E_x) \cdot dE_x}{\int_{-Q}^{E_o} \Phi(E_x) \quad dE_x} \tag{8}$$

where $\phi(E_x)$ is the excitation energy spectrum in ^{6}Li produced from eqs. (5) and (7) at E_{lab}. The upper limit of the integral in the numerator, Eupper, was taken to be Eo if Eo < E_{i+1}, and E_i + 0.25 MeV if Eo ≧ E_{i+1}. The denominator is a normalization constant so as the sum of the cross sections for all the pseudo levels [$\Sigma_i\sigma_i(E_{lab})$] should be equal to the continuum inelastic scattering cross section ($\sigma_c(E_{lab})$) determined in Sect. 2.3.5.

In Fig. 17, some examples of the cross sections for pseudo levels calculated as described in this section are presented. The secondary neutron spectrum in the center-of-mass system is obtained by putting these values in order according to their Q-values. Transformation to the laboratory system is straightforward: it can be done by using the kinematics of the two-body reaction.

The angular distributions for these pseudo levels were assumed to be isotropic in the center-of-mass system.

2.10 Comparison with the Double-Differential Data

In this section, the DDX data produced from the presently evaluated library are compared with the existing experimental data. Typical results are shown in Figs. 18 and 19. These graphs were kindly offered from Dr. Fukahori of JAERI Nuclear Data Center to the authors.

In Fig. 18, the presently evaluated data (histogram) are compared with the data measured at Tohoku University[7] at 14.2 MeV. Generally speaking, the present evaluation reproduces the measured data very well

at all the angular regions. Especially in the high secondary neutron energy region of the forward angles, the present data reproduce the measured ones better than JENDL-3PR1. This is mainly because, in the present evaluation, two higher resonant states at Ex = 4.31 and 5.7 MeV have been newly included.

In Fig. 19, the present data are compared with the data measured by Drosg et al.[63] at 14.1 MeV. At very forward angles, the resolution of their data is not so good and hence the elastic scattering peaks are broad. Even this case, the evaluation is in good agreement with the experimental data.

3. Revision and Status of the Neutron Nuclear Data for ^{7}Li

In JENDL-3PR1, the total, elastic and inelastic scattering, radiative capture, photon-production, (n,2n), (n,d) and (n,n't)α reaction cross sections and the angular and energy distributions of secondary neutrons were evaluated for ^{7}Li[5]. Some data concerning the neutron emitting reactions have been re-evaluated in the present work.

3.1 Total Cross Section

Below 100 keV, the total cross section of ^{7}Li was given by the following expression in JENDL-3PR1:

$$\sigma_{tot} = 0.97 + \sigma_{n,\gamma}$$

where $\sigma_{n,\gamma}$ is the radiative capture cross section. The value 0.97b is the thermal scattering cross section recommended by Mughabghab et al.[50] Below 100 keV, the total cross section was not changed from the JENDL-3PR1 evaluation.

Above 100 keV, the total cross section was evaluated based on the experimental data[15,17,19,20]. The presently was evaluated values are close to the most recent values of Lamaze et al[15]. In this energy range, the total cross section was not changed from JENDL-2.

In Figs. 20-22 shown are the adopted total cross section of ^{7}Li with other evaluated curves and experimental data.

at all the angular regions. Especially in the high secondary neutron energy region of the forward angles, the present data reproduce the measured ones better than JENDL-3PR1. This is mainly because, in the present evaluation, two higher resonant states at Ex = 4.31 and 5.7 MeV have been newly included.

In Fig. 19, the present data are compared with the data measured by Drosg et al.[63] at 14.1 MeV. At very forward angles, the resolution of their data is not so good and hence the elastic scattering peaks are broad. Even this case, the evaluation is in good agreement with the experimental data.

3. Revision and Status of the Neutron Nuclear Data for ^{7}Li

In JENDL-3PR1, the total, elastic and inelastic scattering, radiative capture, photon-production, (n,2n), (n,d) and (n,n't)α reaction cross sections and the angular and energy distributions of secondary neutrons were evaluated for ^{7}Li[5]. Some data concerning the neutron emitting reactions have been re-evaluated in the present work.

3.1 Total Cross Section

Below 100 keV, the total cross section of ^{7}Li was given by the following expression in JENDL-3PR1:

$$\sigma_{tot} = 0.97 + \sigma_{n,\gamma}$$

where $\sigma_{n,\gamma}$ is the radiative capture cross section. The value 0.97b is the thermal scattering cross section recommended by Mughabghab et al.[50] Below 100 keV, the total cross section was not changed from the JENDL-3PR1 evaluation.

Above 100 keV, the total cross section was evaluated based on the experimental data[15,17,19,20]. The presently was evaluated values are close to the most recent values of Lamaze et al[15]. In this energy range, the total cross section was not changed from JENDL-2.

In Figs. 20-22 shown are the adopted total cross section of ^{7}Li with other evaluated curves and experimental data.

3.2 Elastic Scattering Cross Section

As described above, the thermal scattering cross section of 970 mb, recommended by Mughabghab et al.[50], was adopted. Below 100 keV, the elastic scattering cross section was fixed to this value. This part was not changed from JENDL-3PR1.

Above 100 keV, the elastic scattering cross section was given by subtracting the reaction cross section from the total cross section.

Figs. 23 and 24 show the present result. Because in most experiments the inelastic scattering cross section to the first 0.478 MeV level cannot be separated, in those figures also shown are the sum of the elastic and inelastic scattering cross section to the first level by a dashed line. The data of Batchelor and Towle[23], and Knitter[13] do not include the inelastic component and hence are purely elastic scattering. The agreement between the present evaluation and experimental data of Knox et al.[30] is excellent around the resonance at 4.4 MeV.

The angular distribution of elastically scattered neutrons was not changed from JENDL-3PR1 below 14 MeV; below 10 keV it was assumed to be isotropic in the center-of-mass system. Between 10 keV and 4 MeV, it was calculated by the R-matrix theory using the parameters of Knox and Lane[66]. From 4 MeV to 14 MeV, the data in JENDL-2 were adopted.

Above 14 MeV, the elastic scattering angular distribution for ^{7}Li was newly calculated by the coupled-channel theory. The symmetric rotational model was assumed. The coupling scheme was taken as 3/2-(g.s.) - 1/2-(0.478) - 7/2-(4.63) - 5/2-(6.68) (K=1/2 band). The model and the coupling scheme are the same used in the analysis of the ^{7}Li(p,p') reaction by Koori et al[37]. The optical potential and deformation parameters were taken from ref.35.

In Fig. 25, typical results of the presently evaluated angular distributions of elastically scattered neutrons from ^{7}Li are compared with other evaluations and experimental data. In general, the present evaluation reproduces the measured data very well.

3.3 Inelastic Scattering Cross Section

In the present evaluation, two higher excited resonant states at Ex = 6.68 and 7.467 MeV were included as the third and fourth levels in ^{7}Li. Because the particle decay threshold lies at Ex = 2.467 MeV, all

the excited states but the first 0.478 MeV level decay via the $^{7}Li^{*} \rightarrow t+\alpha$ process. Therefore they contribute to the $^{7}Li(n,n't)\alpha$ reaction. The first level decays by emitting γ-rays and it is well known that this γ-ray has an isotropic angular distribution.

3.3.1 The First Level (0.478 MeV)

The cross section was not changed from the JENDL-3PR1 evaluation. In JENDL-3PR1, the $(n,n'\gamma)$ data measured by Morgan et al.[69] were adopted in the whole energy range. The evaluation was performed using the spline function fitting by NDES. The result is shown in Fig. 26.

The angular distribution was revised in the present evaluation. Below 4 MeV it was calculated by the R-matrix theory. Between 4 and 10 MeV, the data evaluated by Liskien[75] based on his experiment on the Doppler-broadened γ-ray spectrum were adopted. Above 10 MeV, the coupled-channel calculation was made.

3.3.2 The Second Level (4.63 MeV)

There is inconsistency among the measured data for this cross section between 7 MeV and 14 MeV. Hogue et al.[29] and Dekempenner et al.[75] give higher values while Hopkins et al.[27], Schmidt et al.[76], Birjukov et al.[67], Lisowski et al.[31], Cookson et al.[26] and Chiba et al.[78] give values considerably smaller than them. In the JENDL-3PR1 evaluation, the data of Hogue et al. were adopted because they span a large energy range from 9 to 14 MeV. In the present evaluation, this cross section was revised taking account of the recent experimental values. The evaluated curve is compared with the experiments in Fig. 27.

In JENDL-3PR1, the angular distribution of inelastically scattered neutrons from this level was assumed to be isotropic in the center-of-mass system. Experiments show, however, that the cross section is strongly forward peaked above several MeV. Hence this part was newly evaluated: below 14 MeV, experimental values[29,38,78] were adopted. Above 14 MeV, the angular distribution was calculated by the coupled-channel method described above.

Some examples of the angular distribution for this level are shown in Fig. 28. In Fig. 29, the present evaluation are compared at 18 MeV with the recent experimental data and other evaluations for $^{7}Li(n,n_0+n_1)$ and (n,n_2) reactions. In this higher energy region, the present evaluation can predict the measured data better than JENDL-3PR1 as seen in

this figure.

3.3.3 The Third Level (6.68 MeV)

This level was newly included in the present evaluation. There are two experimental data at 14 MeV[6,7], although they have not been published. In the present evaluation, the results of the coupled-channel calculation described above were normalized to these data. Angular distribution was also calculated by the coupled-channel method. The result is shown in Fig. 30.

3.3.4 The Fourth Level (7.467 MeV)

This level was newly included in the present evaluation. There are two unpublished data in Japan around 14 MeV[6,7]. In the present evaluation, the excitation function for this level was assumed to be the same as that of the third level except very near the threshold.

Angular distribution for this level was assumed to be isotropic in the center-of-mass system. The result is shown in Fig. 30.

3.3.5 Continuum inelastic scattering

The continuum inelastic scattering in ^{7}Li is due to the reaction ^{7}Li(n,n't)α. The system t + α has some resonances and these resonances were considered as the second, third and fourth levels in ^{7}Li as described above. Therefore, the continuum inelastic scattering cross section was obtained by subtracting these discrete inelastic scattering cross sections from the total ^{7}Li(n,n't)α reaction cross section. The method of evaluating the ^{7}Li(n,n't)α reaction cross section will be described in the next section.

The energy distribution of the continuum neutrons produced by this reaction was calculated by the similar way described in the section 2.9 for ^{6}Li. Replacing d with t, equations (5) and (7) are also applied for ^{7}Li. They are expressed by pseudo levels as similar to ^{6}Li. Thirty levels were necessary to span the energy range from threshold to 20 MeV.

With regard to the angular distribution of these pseudo levels, the angular distribution of continuum neutrons reported in a ref.7 was adopted.

3.4 The $^{7}Li(n,n't)\alpha$ Reaction

After the evaluation of JENDL-3PR1 data, several measurements were reported on this quantity. They all used the tritium accumulation and β-counting method which is considered to be highly reliabe. In the present evaluation, the measurements by D.L. Smith et al.[89], Maekawa et al.[92], Takahashi et al.[10] and Goldberg et al.[91] were newly considered and the cross section was slightly (about 5%) increased in the 14 MeV region compared with the JENDL-3PR1 evaluation. The result is shown in Figs. 31 and 32 by solid lines. In the data files, this cross section is given with the MT number of 205 (MT=205) for users' convenience.

3.5 The $^{7}Li(n,2n)$ Reaction

The JENDL-3PR1 data were not revised for this reaction in the present evaluation. In JENDL-3PR1, the data measured by Ashby et al.[43] and Mather and Pain[44] were adopted at 14 MeV. The result is shown in Fig. 33.

The angular distribution of neutrons emitted from the $^{7}Li(n,2n)$ reaction was replaced by the experimental data[7]. It is given in the laboratory system.

The conventional evaporation model was assumed for the secondary neutron energy distribution. The evaporation temperature (θ) reported in ref.7 was adopted at 14 MeV. This temperature was extrapolated to lower and higher energies according to the relation that θ should be proportional to the square root of the incident neutron energy.

3.6 The $^{7}Li(n,d)$ Reaction

The $^{7}Li(n,d)$ reaction cross section was not revised from the JENDL-3PR1 data. In JENDL-3PR1, this cross section was calculated with DWBA assuming the proton pickup mechanism. As the optical potentials, the neutron parameters of Watson et al.[94] and the deuteron parameters of Bingham et al.[95] were used. The bound state wave-function for the p + ^{6}He system was calculated by the separation energy method with the form factor parameters of: r_0 = 1.25, r_c = 1.25 and a = 0.65 fm. The calculated values were normalized so that the cross section at 14.2 MeV might give a value of 9.8 mb which was obtained by Battat and Ribe[45]. The

result is shown in Fig. 34.

3.7 Radiative Capture Cross Section

The data in JENDL-3PR1, which are the same as those in JENDL-2, were adopted without any revision. They are expressed as

$$\sigma_{n,\gamma} = 7.22 \times 10^{-3} \, [En(eV)]^{-1/2} \quad \text{(barns)} \tag{9}$$

The result is shown in Fig. 35.

3.8 Photon Production Cross Section

This cross section was not changed from the JENDL-3PR1 evaluation. It includes the contribution from the $^{7}Li(n,n_1)^{7}Li^*$ and radiative capture reactions. Because the threshold for the particle decay is very low (Ex = 2.467 MeV), all the excited states except the first level decay by emitting particles prior to γ-ray transition.

3.8.1 The $(n,n_1\gamma)$ Reaction

The γ-rays emitted from this reaction have a probability of 100% and an isotropic angular distribution. Therefore, a value of 1.0 was given to the multiplicity.

3.8.2 The (n,γ) Reaction

The multiplicites for capture γ-rays were deduced from the γ-ray intensities measured by Jurney[60] at the thermal energy. The result is the following:

Transition	Multiplicity
cap. → g.s.	0.894
cap. → 0.98 MeV	0.106
0.98 MeV → g.s.	0.106

The angular distributions of the γ-rays were assumed to be isotropic.

3.9 Comparison with the Double-Differential Data

The presently evaluated data were compared with some of the existing DDX data and are shown in Figs. 36-38.

In Fig. 36 the presently evaluated curve is compared with the data measured at Osaka University[6] around 14 MeV using a natural lithium sample. The present evaluation reproduces the experimental data very well from forward angles to backward angles. Especially in the secondary neutron energy region just below the 4.64 MeV state, the agreement is considerably improved. This is because in the present evaluation, two higher excited states at Ex = 6.68 and 7.476 MeV were included.

In Fig. 37 the present data are compared with the data taken at Tohoku University at 14.2 MeV[7]. This experiment was made using an isotopically enrich sample (99.9% in ^{7}Li). Generally speaking, the agreement between the present evaluation and experimental data is also excellent including the valley just below the elastic peak.

In Fig. 38, the present results are plotted with the measured data[7] at 6.0 MeV. In the experimental results, the elastic scattering peak was already subtracted. Agreement between the evaluated and measured data is satisfactory. The structures seen in the evaluated data arise from the discretization of the continuum neutrons with a 0.5 MeV interval in excitation energy.

4. Concluding Remarks

The neutron nuclear data ^{6}Li and ^{7}Li, stored in JENDL-3PR1, were revised for JENDL-3 by taking account of the experimental data measured after the evaluations. Much empahsis was placed on the double-differential neutron emission cross section data. The ^{7}Li(n,n't)α reaction cross section was also revised, and it was increased slightly around 14 MeV according to the recent measurements using the tritium counting method.

The spectrum of the continuum secondary neutrons produced by the ^{6}Li(n,n'd)α and ^{7}Li(n,n't)α reactions were calculated by the three-body phase-space model with the Coulomb interaction between the two unobserved particles. In the evaluated files, they were described by the pseudo-level representation with a 0.5 MeV interval. The secondary neutron spactra from the ^{6}Li and ^{7}Li(n,2n) reactions were given by the conven-

3.9 Comparison with the Double-Differential Data

The presently evaluated data were compared with some of the existing DDX data and are shown in Figs. 36-38.

In Fig. 36 the presently evaluated curve is compared with the data measured at Osaka University[6] around 14 MeV using a natural lithium sample. The present evaluation reproduces the experimental data very well from forward angles to backward angles. Especially in the secondary neutron energy region just below the 4.64 MeV state, the agreement is considerably improved. This is because in the present evaluation, two higher excited states at Ex = 6.68 and 7.476 MeV were included.

In Fig. 37 the present data are compared with the data taken at Tohoku University at 14.2 MeV[7]. This experiment was made using an isotopically enrich sample (99.9% in ^{7}Li). Generally speaking, the agreement between the present evaluation and experimental data is also excellent including the valley just below the elastic peak.

In Fig. 38, the present results are plotted with the measured data[7] at 6.0 MeV. In the experimental results, the elastic scattering peak was already subtracted. Agreement between the evaluated and measured data is satisfactory. The structures seen in the evaluated data arise from the discretization of the continuum neutrons with a 0.5 MeV interval in excitation energy.

4. Concluding Remarks

The neutron nuclear data ^{6}Li and ^{7}Li, stored in JENDL-3PR1, were revised for JENDL-3 by taking account of the experimental data measured after the evaluations. Much empahsis was placed on the double-differential neutron emission cross section data. The ^{7}Li(n,n't)α reaction cross section was also revised, and it was increased slightly around 14 MeV according to the recent measurements using the tritium counting method.

The spectrum of the continuum secondary neutrons produced by the ^{6}Li(n,n'd)α and ^{7}Li(n,n't)α reactions were calculated by the three-body phase-space model with the Coulomb interaction between the two unobserved particles. In the evaluated files, they were described by the pseudo-level representation with a 0.5 MeV interval. The secondary neutron spactra from the ^{6}Li and ^{7}Li(n,2n) reactions were given by the conven-

tional evaporation model. Two higher resonant states, which had not been included in the JENDL-3PR1 evaluation, were included in the present evaluation. A coupled-channel calculation was performed to interpolate and extrapolate the elastic and some inelastic scattering cross sections. The present results were compiled in the ENDF/B-V format.

Aknowledgements

The authors would like to thank Dr. S. Igarasi for his helpful discussion and advice throughout the work. They are also grateful to Dr. T. Nagakawa for his advice in making data files, Mr. T. Narita for his aid in making graphs and to Dr. T. Fukahori for presenting graphs on DDX. They are also indebted to Drs. Y. Kawarasaki and M. Mizumoto for helpful comments and encouragement. The advice from Drs. M. Baba, K. Kanda and N. Hirakawa of Tohoku University is also appreciated very much.

tional evaporation model. Two higher resonant states, which had not been included in the JENDL-3PR1 evaluation, were included in the present evaluation. A coupled-channel calculation was performed to interpolate and extrapolate the elastic and some inelastic scattering cross sections. The present results were compiled in the ENDF/B-V format.

Aknowledgements

The authors would like to thank Dr. S. Igarasi for his helpful discussion and advice throughout the work. They are also grateful to Dr. T. Nagakawa for his advice in making data files, Mr. T. Narita for his aid in making graphs and to Dr. T. Fukahori for presenting graphs on DDX. They are also indebted to Drs. Y. Kawarasaki and M. Mizumoto for helpful comments and encouragement. The advice from Drs. M. Baba, K. Kanda and N. Hirakawa of Tohoku University is also appreciated very much.

References

1) Shibata K. and Kikuchi Y. : Radiation Effects, 96, 243 (1986).
2) Nakagawa T. (Ed.) : "Summary of JENDL-2 General Purpose File", JAERI-M 84-103 (1984).
3) Kikuchi Y., Shibata K., Asami T., Sugi T., Yamakoshi H. and Kitajima N. : Jour. Nucl. Sci. Technol., 22, 499 (1985).
4) Shibata K. : "Evaluation of Neutron Nuclear Data of ^{6}Li for JENDL-3", JAERI-M 84-198 (1984).
5) Shibata K. : "Evaluation of Neutron Nuclear Data of ^{7}Li for JENDL-3", JAERI-M 84-204 (1984).
6) Takahashi A. : "Double Differential Neutron Emission Cross Sections at 14 MeV Measured at OKATAVIAN", Proc. of Specialists' Meeting on Nuclear Data of Fusion Neutronics, JAERI-M 86-029, 99 (1986).
7) Chiba S., Baba M., Nakashima H., Ono M., Yabuta N. Yukinori S. and Hirakawa N. : Jour. Nucl. Sci. Technol., 22, 771 (1985).
8) Hashikura H., Oka Y. and Kondo S. : "Comparison between Measurements of the Neutron Spectra from Materials used in Fusion Reactors and Calculations using JENDL-3PR1", Proc. of Specialists' Meeting on Nuclear Data of Fusion Neutronics, JAERI-M 86-029, 160 (1986).
9) Sugiyama K., Kanda K., Iwasaki S., Nakazawa M., Hashikura H., Iguchi T., Sekimoto H., Itoh S., Sumita K., Takahashi A. and Yamamoto J. : "Neutronic Experiments in a 120 cm Lithium Sphere", Proc. 13th SOFT on September 24-28, 1984, at Varese, Italy, p1375 (1984).
10) For example, Takahashi A., Yugami K., Kohno K., Ishigaki N., Yamamoto J. and Sumita K. : Proc. 13th Symp. Fusion Technology, Padua, Italy, September 1984, p.1325, Pergamon Press, Oxford (1984).
11) Komoda S., Shibata K., Chiba S. and Igarasi S. : RESCAL, to be published.
12) Smith A.B., Guenther P., Havel D. and Whalen J.F. : "Note on the 250 keV Resonance in the Total Neutron Cross Section of ^{6}Li", ANL/NDM-29 (1979).
13) Knitter H.H., Budtz-Jorgensen C., Mailly M. and Vogt R. : "Neutron Total and Elastic Scattering Cross Sections of ^{6}Li in the Energy Range from 0.1 to 3.0 MeV", EUR 5726e (1977).
14) Macklin R.L., Ingle R.W. and Halperin J. : Nucl. Sci. Eng., 71, 205 (1979).
15) Lamaze G.P., Kellie J.D. and Schwartz R.B. : Bull. Am. Phys. Soc.,

24, 862 (1979).

16) Guenther P., Smith A.B. and Whalen J. : "Neutron Total and Scattering Cross Section of ^{6}Li in the Few MeV Region", ANL/NDM-52 (1980).

17) Foster, Jr. D.G. and Glasgow D.W. : Phys. Rev., C3, 576 (1971).

18) Meadows J.W. and Whalen J.F. : Nucl. Sci. Eng., 48, 221 (1972).

19) Goulding C.A. and Stoler P. : "Total Neutron Cross Section of ^{4}He, ^{6}Li and ^{7}Li From 0.5 to 30 MeV", USNDC-3, 161 (1972).

20) Harvey J.A. and Hill N.W. : "Neutron Total Cross Section of ^{6}Li from 10 eV to 10 MeV", Proc. Fourth Conf. Nuclear Cross-Sections and Technology, Washington 1975, 244 (1975).

21) Nakagawa T. : "NDES ; Neutron Data Evaluation System", in J. At. Energy Soc. Jpn., 22, 559 (1980) (in Japanese).

22) Alfimenkov et al. : YF 36(5) 1089 (1982), EXFOR40659002.

23) Batchelor R. and Towle J.H. : Nucl. Phys., A47, 385 (1963).

24) Armstrong A.H., Gammel J. and Rosen L. : Nucl. Phys., A52, 505 (1964).

25) Merchez F., Regis V., Nguyen V.S., Darves-Blanc R., Pham D.L. and Bouchez R. : de Phys. Colloque 27, 1 (1966).

26) Cookson J.A., Dandy D. and Hopkins J.C. : Nucl. Phys., A91, 273 (1967).

27) Hopkins J.C., Drake D.M. and Conde H. : Nucl. Phys., A107, 139 (1968).

28) Abbondanno M. and Poiani G. : Nuovo Cimento A66, 139 (1970).

29) Hogue H.H., von Behren P.L., Glasgow D.W., Glendinning S.G., Lisowski P.W., Nelson C.E., Purser F.O., Tornow W., Gould C.R. and Seagondollar L.W. : Nucl. Sci. Eng., 69, 22 (1979).

30) Knox H.D., White R.M. and Lane R.O. : Nucl. Sci. Eng., 69, 223, (1979).

31) Lisowski P.W., Auchampaugh G.F., Drake D.M., Drosg M., Haouat G., Hill N.W. and Nilsson L. : "Cross Sections for Neutron-Induced, Neutron-Producing Reactions in ^{6}Li and ^{7}Li at 5.96 and 9.83 MeV", LA-8342 (1980).

32) Fortsch H., Schmidt D., Seeliger D. and Streil T. : "Messung von Neutronenstreuquerschnitten der Nuklide ^{6}Li and ^{7}Li bei Einschussenergien E_0 = 7 bis 10 MeV", ZfK-443, 13 (1981).

33) Lane R.O. et al. : EUR-3454E (1967), EXFOR 20376003.

34) Raynal J. : "Notes on ECIS79", unpublished.

35) Chiba S., Baba M., Nakashima H., Ono M., Yabuta, N. Yukinori, S. and Hirakawa N. : Radiation Effects, 92, 227 (1986).

36) Hansen L.F., Haight R.C., Pohl B.A., Wong C. and Lagrange Ch. : "Neutron Scattering on Deformed Nuclei", UCRL-91217 (1984).

37) Koori N., Kumabe I., Hyakutake M., Orito K., Akagi K. and Watanabe Y. : "Measurement of ^{7}Li(p,p') and (p,t) Reaction Induced by Polarized Protons of 12, 14 and 16 MeV", KUNE report 87-1 (1987).

38) Hyakutake M., Sonoda M., Katase A., Wakuta Y., Matoba M. Tawara H. and Fujita I. : J. Nucl. Sci. Technol., 11, 407 (1974).

39) Presser G., Bass R. and Kruger K. : Nucl. Phys., A131, 679 (1969).

40) Besotosnyj, Gorbachev, Suvorov and Shvetsov : YK-19, 77 (1975).

41) Drake D.M. : "Cross Sections for Neutron-Induced, Neutron-Producing Reactions in ^{6}Li and ^{7}Li at 14.1 MeV", BNL-NCS-29426, 71 (1981).

42) Rosen L. and Stewart L. : Phys. Rev., 126, 1150 (1962).

43) Ashby V.J., Catron H.C., Goldberg M.D., Hill R.W., LeBlanc J.M., Newkirk L.L., Stoering J.P., Taylor C.J. and Williamson M.A. : Phys. Rev., 129, 1771 (1963).

44) Mather D.S. and Pain L.F. : "Measurmenet of (n,2n) and (n,3n) Cross Sections at 14 MeV Incident Energy", AWRE-O-47/69 (1969).

45) Battat M.E. and Ribe F.L. : Phys. Rev., 89, 80 (1953).

46) Frye, Jr. G.M. : Phys. Rev., 93, 1086 (1954).

47) Schantl W., EXFOR 21846001 (1970).

48) Prasad R. and Sarkar D.C. : Nuovo Cimento, A3, 467 (1971).

49) Merchez F., Bouchez R. and Yavin A.I. : Nucl. Phys., A182, 428 (1972).

50) Mughabghab S.F., Divadeenam M. and Holden N.E. : "Neutron Cross Sections Vol.1", Academic Press, 1981.

51) Bartle C.M. : Nucl. Phys., A330, 1 (1979).

52) Bartle C.M., Gebbie D.W. and Hollas C.L. : Nucl. Phys., A397, 21 (1983).

53) Friesenhahn S.J., Orphan V.J., Carlson A.D., Fricke M.P. and Lopez W.M. : "The (n,α) Cross Sections of ^{6}Li and ^{10}B Between 1 and 1500 keV", INTEL-Rt 7011-001, Intelcom Rac. Tech. (1974).

54) Fort E. and Marquette J.P. : "Etude de la Section Efficace ^{6}Li(n,α)T dans Gamme d'Energie Comprise entre 20 keV et 1700 keV:, EANDC(E)-148 (1972).

55) Coates M.S., Hunt G.J. and Uttley C.A. : "Measurement of Standard Cross-Sections using the Harwell Black Detector", EANDC(UK)-151, 10 (1973).

56) Poenitz W.P. : Z. Phys., 268, 359 (1974).

57) Lamaze G.P., Schrack R.A. and Wasson O.A. : Nucl. Sci. Eng., 68, 183 (1978).

58) Renner C., Harvey J.A., Hill N.W., Morgan G.L. and Rush K. : Bull.

Am. Phys. Soc. 23, 526 (1978).

59) Ferdinande H., Sherman N.K., Lokan K.H. and Ross C.K. : Can. J. Phys., 55, 428 (1977).

60) Jurney E.T. : "Thermal Capture Cross Sections for ^{6}Li and ^{7}Li", USNDC-9, 109 (1973).

61) Gillespie J. : "Final-State Interactions", Holden-Day, 1964.

62) Holland R.D., Elwyn A.J., Davids C.N., Lynch F.J., Meyer-Schutzmeister L., Monahan J.E., Mooring F.P. and Ray, Jr. W. : Phys. Rev., 19, 592 (1979).

63) Drosg M. : Radiation Effects, 92, 145 (1986).

64) Meadows J.M. and Whalen J.F. : Nucl. Sci. Eng. 41, 351 (1970).

65) Harvey J.A. et al. DOE-NDC-12, 229 (1978), EXFOR12876002.

66) Knox H.D. and Lane R.O. : Nucl. Phys., A359, 131 (1981).

67) Birjukov N.S., Zhuravljov B.V., Kornilov N.V., Popov V.I., Rudenko A.P., Salnikov O.A. and Trykove V.I. : "Scattering of 9.1 ± 0.2 MeV neutrons by Li-7 Nuclei", Proc. Fourth All Union Conf. Neutron Physics, Kiev 1977, Vol.2, 27 (1977).

68) Baba M., Hayashi N., Sakase T., Iwasaki T., Kamata S. and Momota T. : "Neutron Scattering from ^{7}Li at Incident Energies of 5.1, 6.6 and 15.4 MeV", Proc. Int. Conf. Nuclear Cross Sections for Technology, Knoxville 1979, 43 (1980).

69) Morgan G.L. : "Cross Sections for the ^{7}Li(n,xn) and ^{7}Li(n,n'γ) Reactions between 1 and 20 MeV", ORNL/TM-6247 (1978).

70) Benveniste J., Mitchell A.C., Shrader C.D. and Zenger J.H. : Nucl. Phys., 38, 300 (1962).

71) Freeman : Phil. Mag. 46, 17 (1955).

72) Presser G. and Bass R. : Nucl. Phys., A182, 321 (1972).

73) Smith D.L., Bretscher M.M. and Meadows J.W. : Nucl. Sci. Eng., 78, 359 (1981).

74) Olsen D.K., Morgan G.L. and McConnell J.W. : Nucl. Sci. Eng., 74, 219 (1980).

75) Liskien H. : Private Communication.

76) Dekempeneer E., Liskien H., Mewissen L. and Poortmans F. : Nucl. Sci. Eng., 97, 353 (1987).

77) Schmidt D., Seeliger D., Lovchikova G.N. and Trufanov A.M. : Nucl. Sci. Eng., 96, 159 (1987).

78) Ferch G., Schmidt D., Zeliger D., Shtrail T., Lovchikova G.N. and Trufanov A.M. : "Elastic and Inelastic Scattering Cross Section for

^{6}Li and ^{7}Li Nuclei at an Initial Energy of 8.9 MeV", INDC (CCP)-221, L, 18 (1984).

79) Chiba S., Yamanouti Y., Mizumoto M., Hyakutake M. and Iwasaki S., Jour. Nucl. Sci. Technol., 25, 210 (1988).

80) Chiba S., Baba M., Kikuchi T., Ishikawa M., Hirakawa N. and Sugiyama K. : "Measurement of Neutron-Induced Neutron-Producing Cross Sections of ^{6}Li and ^{7}Li at 18.0 MeV", presented at the Int. Conf. on Nuclear Data for Science and Technology, May 30 - June 3, 1988, Mito.

81) Qaim S.M. and Wolfle R. : Nucl. Sci. Eng., 96, 52 (1987).

82) Maekawa H., Tsuda K., Iguchi T., Ikeda Y., Oyama Y., Fukumoto T., Seki Y. and Nakamura T. : "Measurements of tritium production-rate distribution in simulated blanket assemblies at the FNS", JAERI-M 83-196 (1983).

83) Swinhoe M.T. and Uttley C.A. : Nucl. Sci. Eng., 89, 261 (1985).

84) Liskien H. and Paulsen A. : Ann. Nucl. Energy, 8, 423 (1981).

85) Liskien H., Wolfle R. and Qaim S.M. : "Determination of ^{7}Li(n,n't)^{4}He cross sections", Proc. Int. Conf. on Nuclear Data for Science and Technology, Antwerp 1982, 349 (1983).

86) Thomas R.G. Walt M., Walton R.B. and Allen R.C. : Phys. Rev. 101, 759 (1956).

87) Brown F., James R.H., Perkin J.L. and Barry J. : Reactor Sci. Technol. (J. Nucl. Ener., A/B), 17, 137 (1963).

88) Wyman M.E. and Thorpe, M.M. : "A measurement of the ^{7}Li(n,alpha)t cross section for several neutron energies", LA-2235, (1958).

89) Osborn : "The cross section for the ^{7}Li(n,n+t) reaction", AWRE-NR/C-1, (1961).

90) Smith D.L., Meadows J.W., Bretsher M.M. and Cox S.A. : "Cross-section measurement for the ^{7}Li(n,n't)^{4}He reaction at 14.74 MeV", ANL/NDM-87, (1984).

91) Swinhoe M.T. : Value reported in ANL/NDM-87 (1984), EXFOR12907002.

92) Goldberg E., Barber R.L., Barry P.E., Bonner N.A., Fontanilla J.E., Griffin C.M., Haight R.C., Nethaway D.R. and Hudson G.B. : Nucl. Sci. Eng., 91, 173 (1985).

93) Maekawa H. : Private Communication (1986).

94) Mctaggart : "Shell Transmission Measurements on Lithium", ACO/UK-1337 (1961).

95) Watson B.A., Singh P.P. and Segel R.E. : Phys. Rev., 182, 977 (1969).

96) Bingham H.G., Zander A.R., Kemper K.W. and Fletcher N.R. : Nucl. Phys., A173, 265 (1971).

Table 1 Status of the presently revised quantities (will continue)

^{6}Li

Quantities	Energy range (eV)* min	max	Comments
a) Cross Sections			
Elastic scattering	6.61+6	2.0 +7	Figs. 4, 5
(n,2n)	6.61+6	2.0 +7	Fig. 11
Inelastic scattering			
to the 3rd level	5.03+6	2.0 +7	
to the 4th level	6.66+6	2.0 +7	
to the continuum levels	1.75+6	2.0 +7	Fig. 17 Pseudo levels
b) Angular distributions of secondary neutrons			
Elastic scattering	1.5 +7	2.0 +7	
Inelastic scattering			
to the 1st level	1.5 +7	2.0 +7	
to the 3rd level	5.03+6	2.0 +7	
to the 4th level	6.66+6	2.0 +7	
to the continuum levels	1.75+6	2.0 +7	Pseudo levels
(n,2n)	6.61+6	2.0 +7	
c) Energy distributions of secondary neutrons			
Inelastic scattering to the continuum levels	1.72+6	2.0 +7	
(n,2n)	6.61+6	2.0 +7	Evaporation model

* 2.0+7 denotes 2.0×10^{7}

Table 1 (continued)

^{7}Li

Quantities	Energy range (eV) min	Energy range (eV) max	Comments
a) Cross Sections			
Elastic scattering	1.0 +7	2.0 +7	Fig. 24
Inelastic scattering			
to the 2nd level	5.3 +6	2.0 +7	Fig. 27
to the 3rd level	7.63+6	2.0 +7	
to the 4th level	8.53+7	2.0 +7	
to the continuum levels	1.0 +7	2.0 +7	Pseudo levels
(n,n't)α	1.0 +7	2.0 +7	Figs. 30, 31
b) Angular distributions of secondary neutrons			
Elastic scattering	1.5 +7	2.0 +7	Fig. 29
Inelastic scattering			
to the 1st level	5.46+5	2.0 +7	Fig. 29
to the 2nd level	5.3 +6	2.0 +7	Fig. 28
to the 3rd level	7.63+6	2.0 +7	Fig. 30
to the 4th level	8.53+6	2.0 +7	Fig. 30
to the continuum levels	2.82+6	2.0 +7	
(n,2n)	8.3 +6	2.0 +7	
c) Energy distributions of secondary neutrons			
Inelastic scattering to the continuum levels	1.72+6	2.0 +7	
(n,2n)	6.61+6	2.0 +7	Evaporation model

Table 2 R-matrix parameters used in the n + ^{6}Li analysis.

$J\pi$	$E_\lambda^{J\pi}$	ℓ_n	$\gamma_{\lambda n}^{J\pi}$	$R_{n0}^{\infty J\pi}$	$\gamma_{\lambda n}^{J\pi}$	$R_{n0}^{\infty J\pi}$	ℓ_α	$\gamma_{\lambda\alpha}^{J\pi}$
			(s = 1/2)		(s = 3/2)			
1/2+		0		0.001				
3/2+	1.930	0			1.180	0.0	2	0.460
3/2-	3.430	1	0.875	0.500	1.250	0.200		
5/2-	-0.644	1			0.041	0.0	3	0.429
5/2-	0.212	1			1.000	0.0	3	0.190

$a_n = a_\alpha = 3.853$ fm. $E_\lambda^{J\pi}$ in MeV, $\gamma_{\lambda c}^{J\pi}$ in MeV$^{1/2}$.

The R-matrix is given by

$$R_{c',c}^{J\pi} = R_{c0}^{\infty J\pi}\delta_{c',c} + \sum_\lambda \gamma_{\lambda c'}^{J\pi}\gamma_{\lambda c}^{J\pi}/(E_\lambda^{J\pi} - E).$$

The symbol s denotes the channel spin.

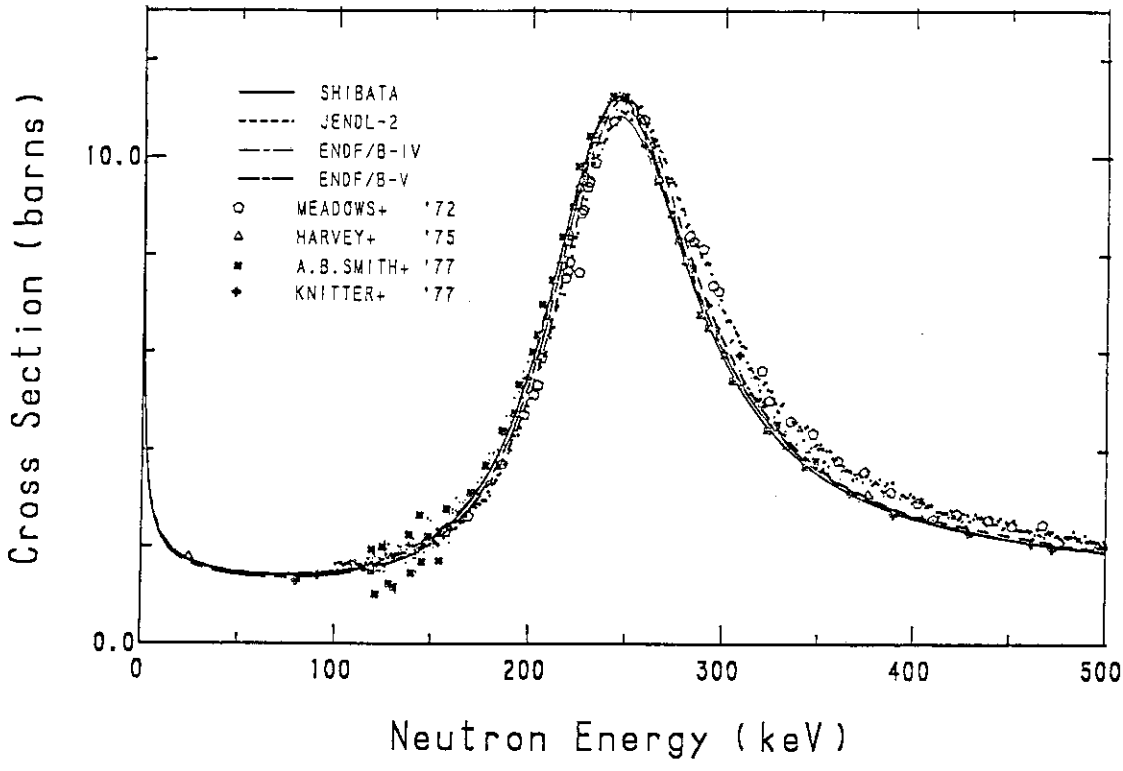

Fig. 1 The Total Cross Section of ^{6}Li (0 ～ 500 keV)

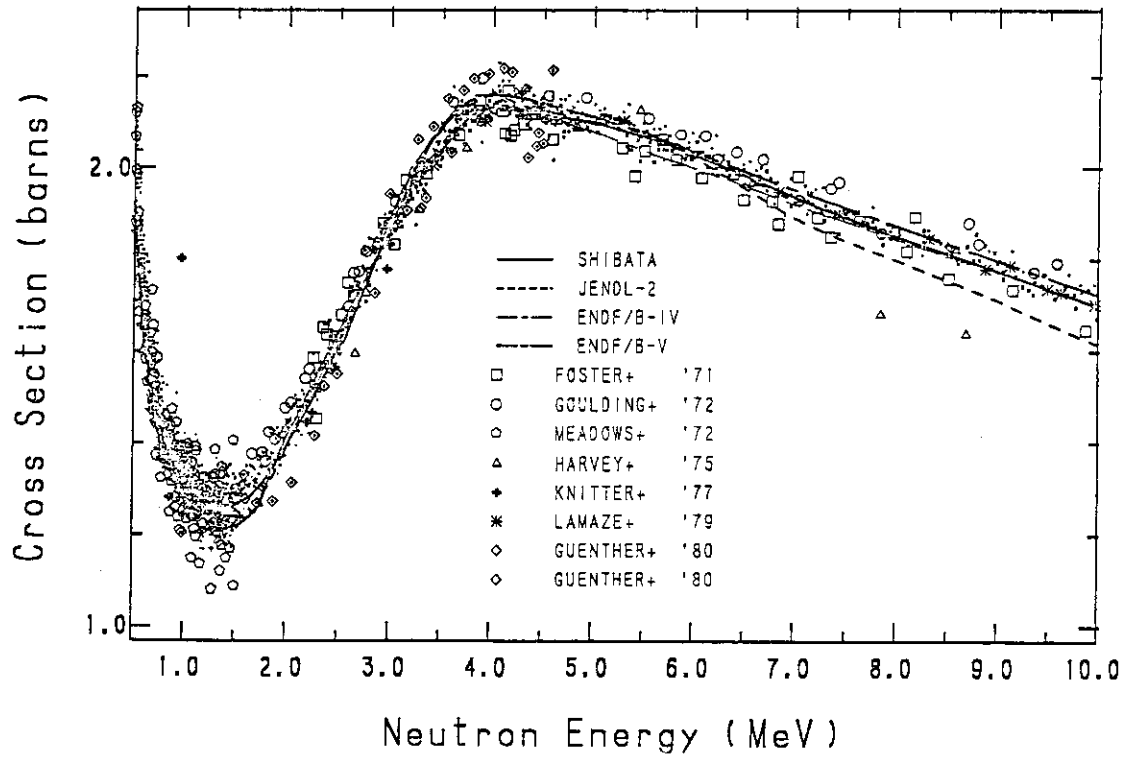

Fig. 2 The Total Cross Section of ^{6}Li (500 keV ～ 10 MeV)

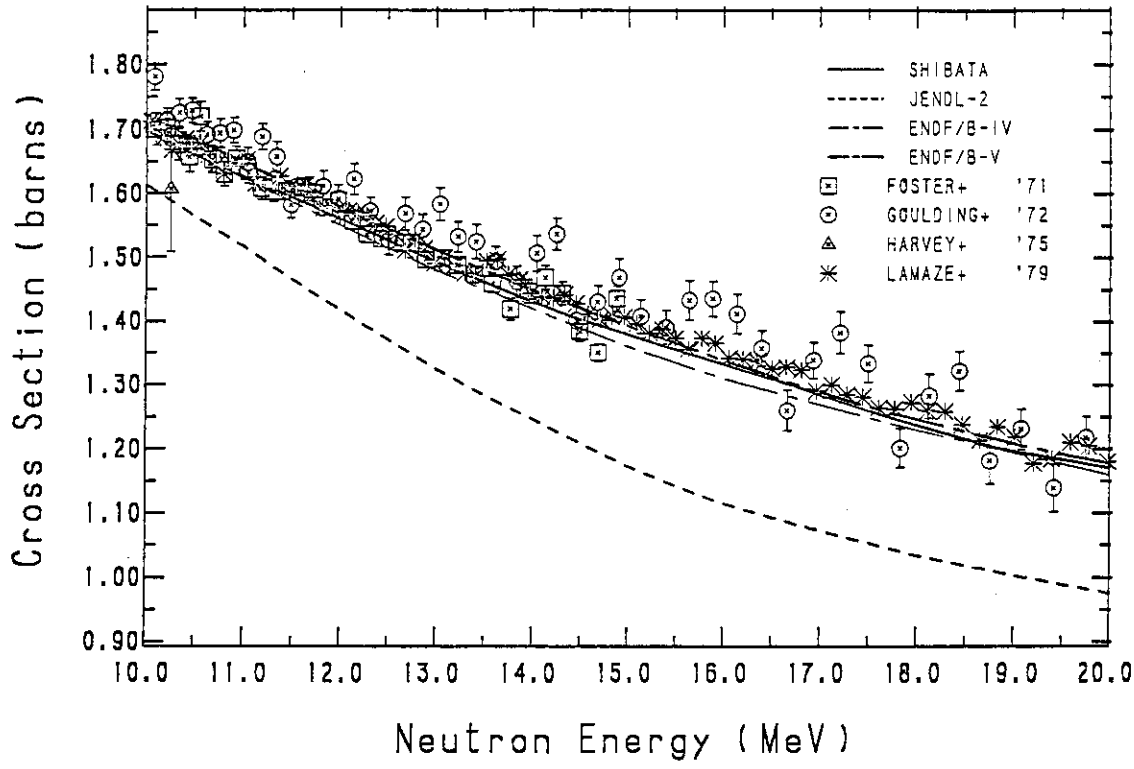

Fig. 3 The Total Cross Section of ^{6}Li (10 ～ 20 MeV)

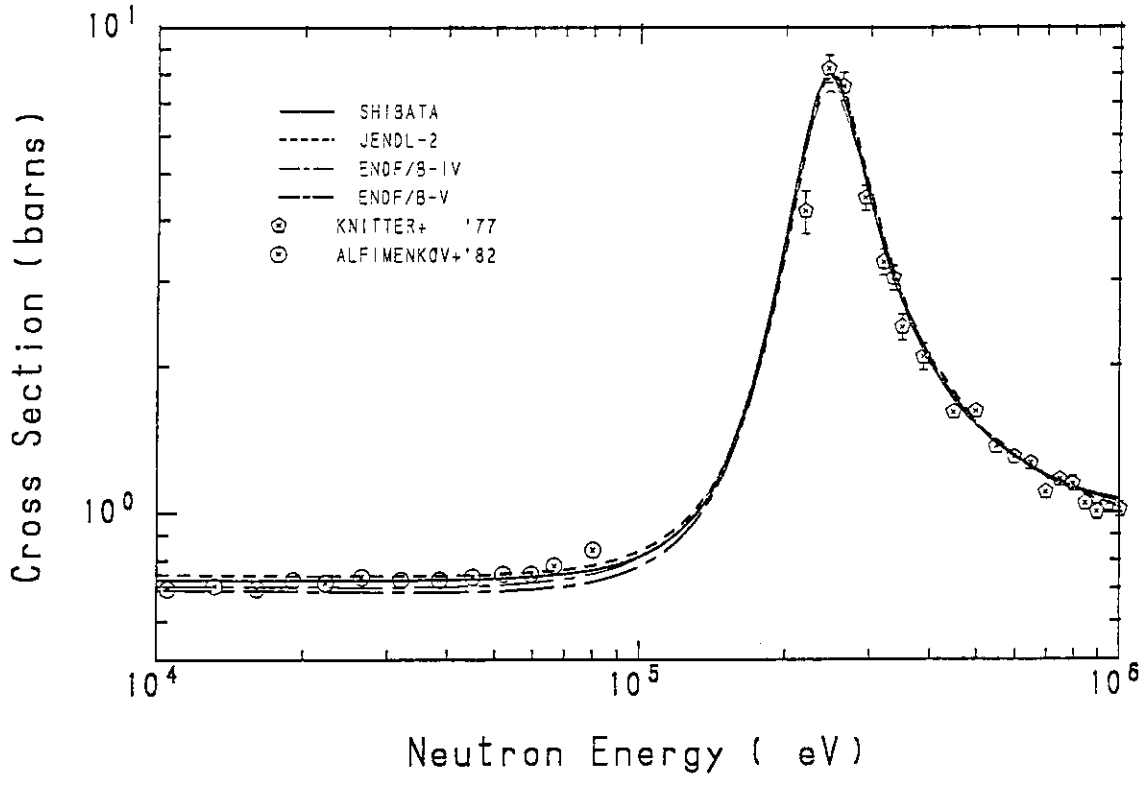

Fig. 4 The Elastic Scattering Cross Section of ^{6}Li

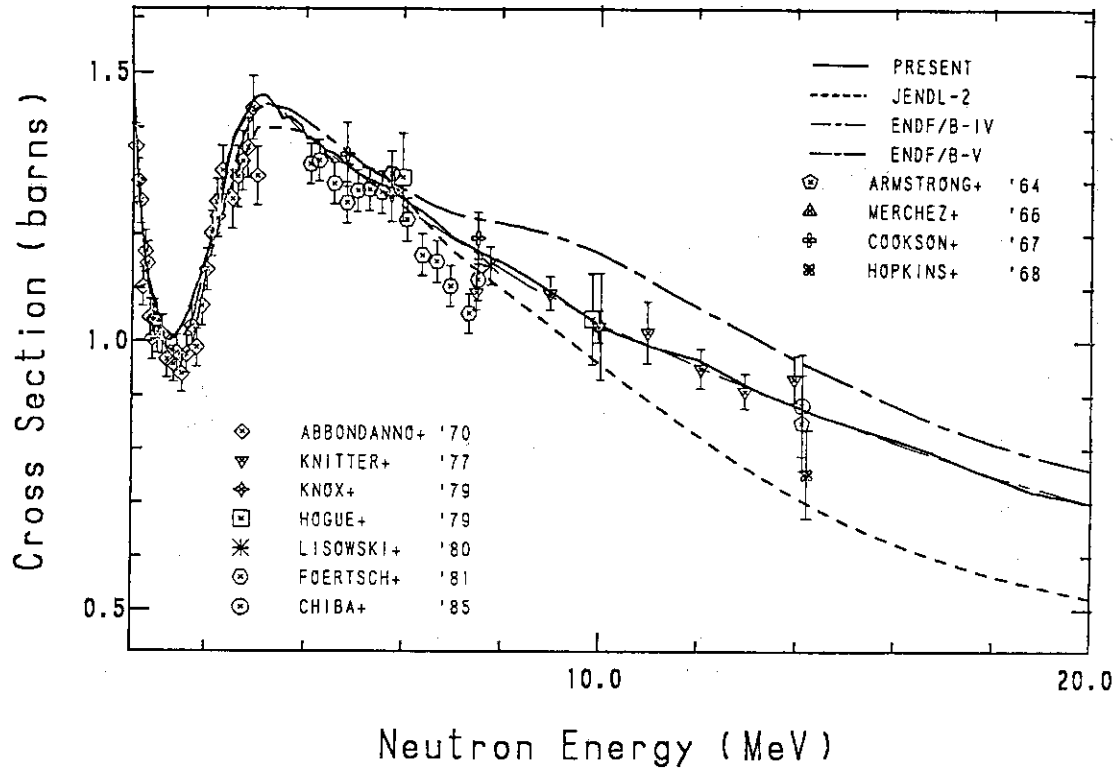

Fig. 5 The Elastic Scattering Cross Section of ^{6}Li

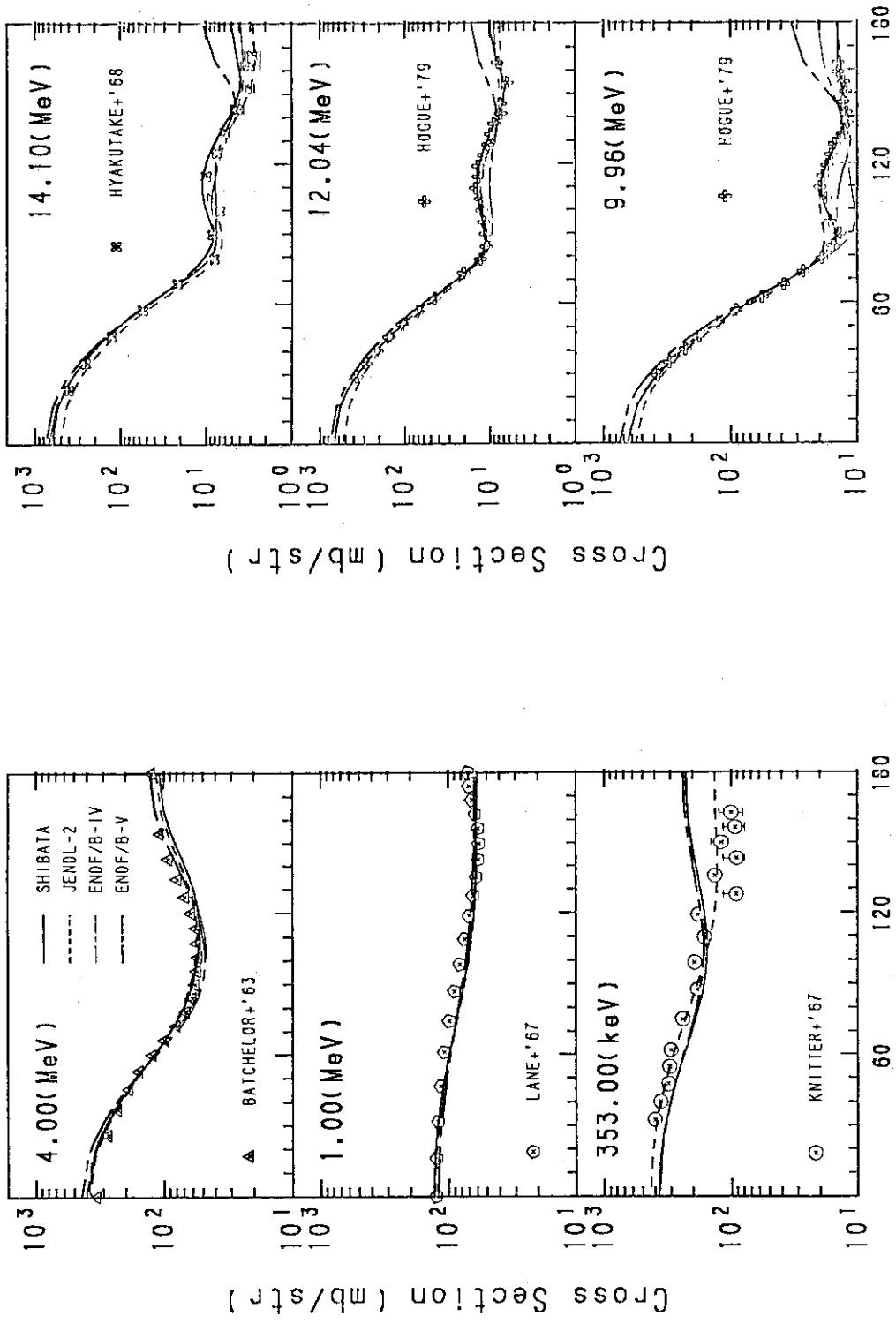

Fig. 6 Angular Distribution of Elastically Scattered Neutrons From ^{6}Li

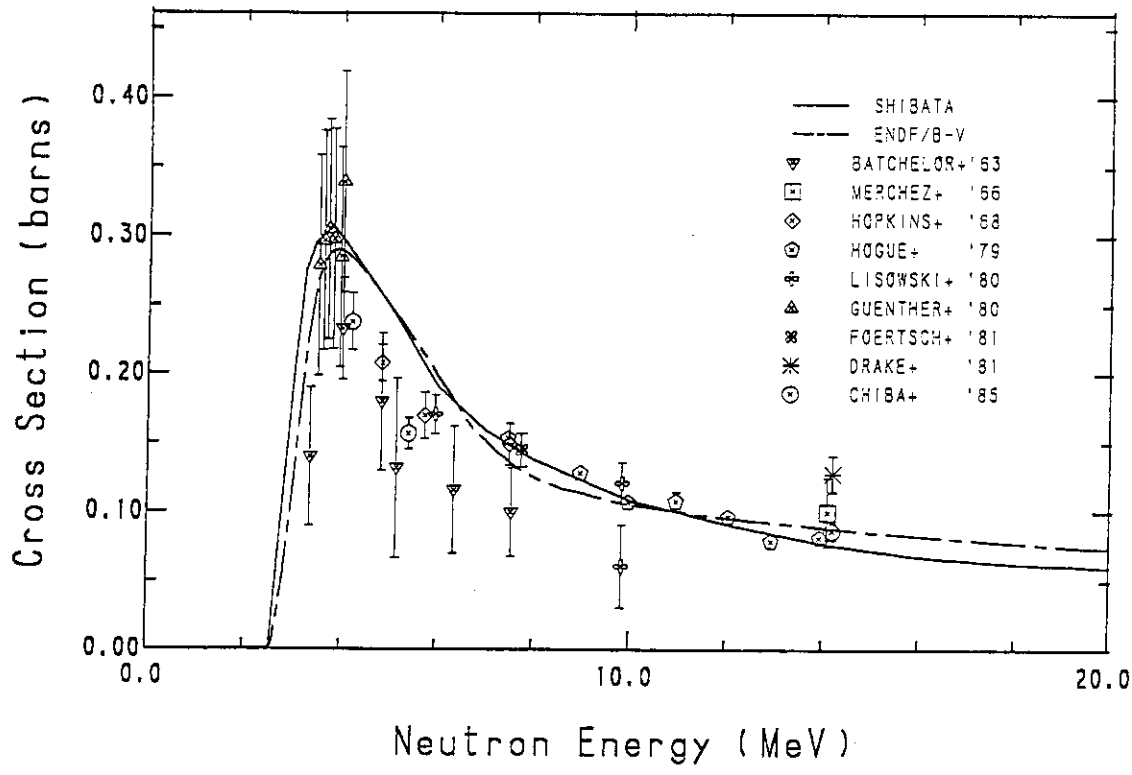

Fig. 7 The $^{6}Li(n,n')^{6}Li^{*}$(2.185 MeV) Cross Section

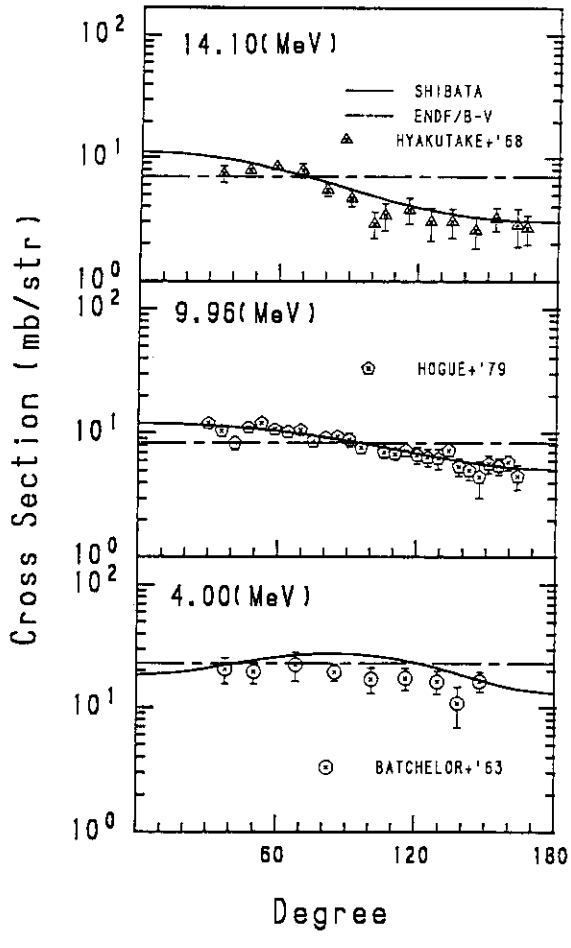

Fig. 8 Angular Distributions of Inelastically Scattered Neutrons from the Second (2.185 MeV) level of ^{6}Li

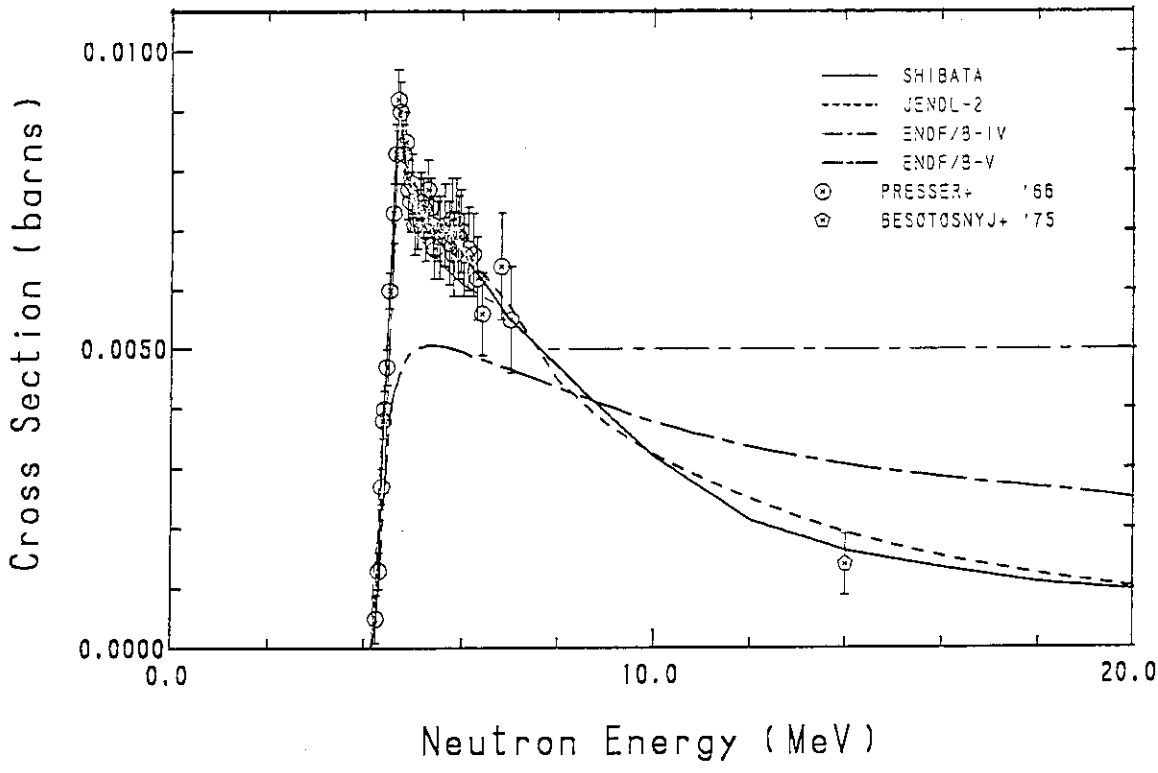

Fig. 9 The $^{6}Li(n,n')^{6}Li^{*}$(3.562 MeV) Cross Section

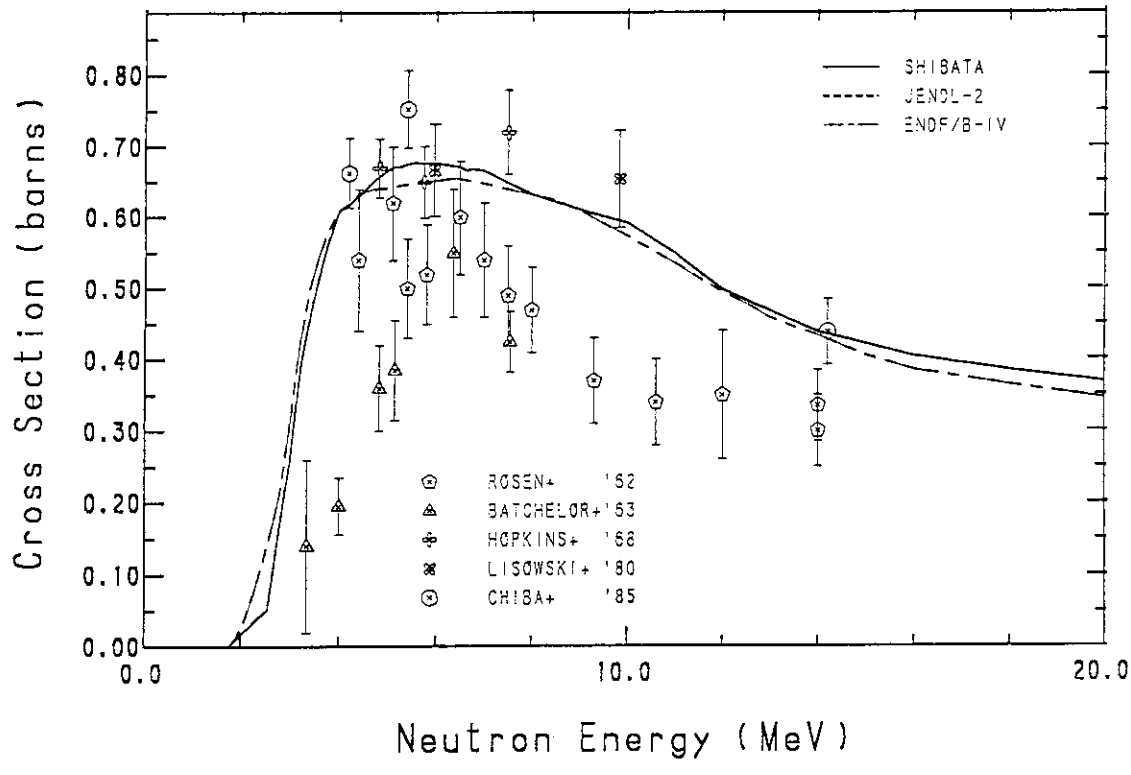

Fig. 10 The $^{6}Li(n,n'd)\alpha$ Reaction Cross Section

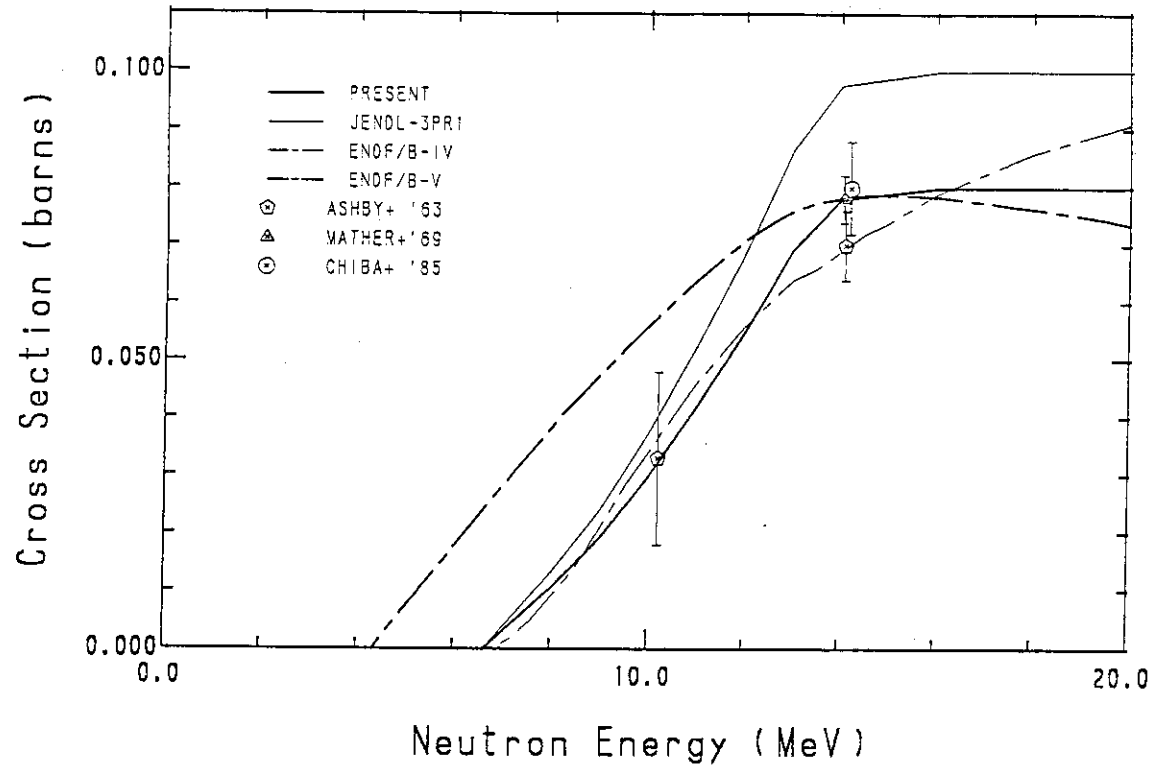

Fig. 11 The $^{6}Li(n,2n)$ Reaction Cross Section

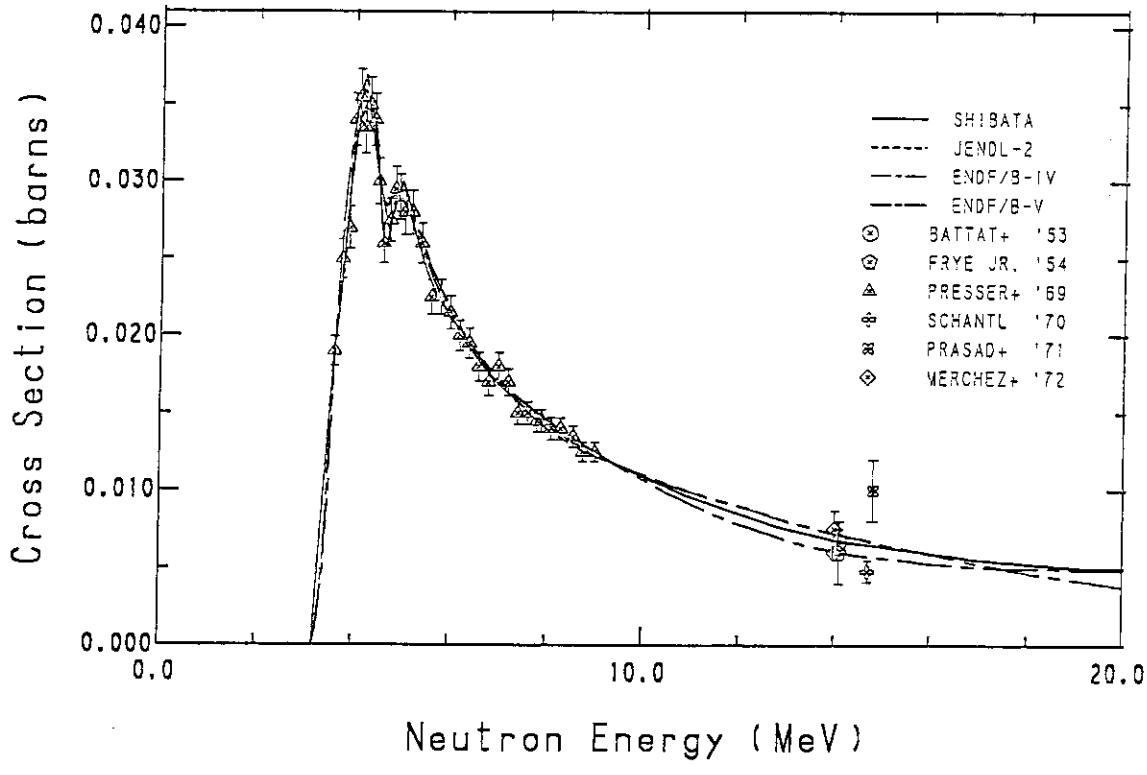

Fig. 12 The $^{6}Li(n,p)$ Reaction Cross Section

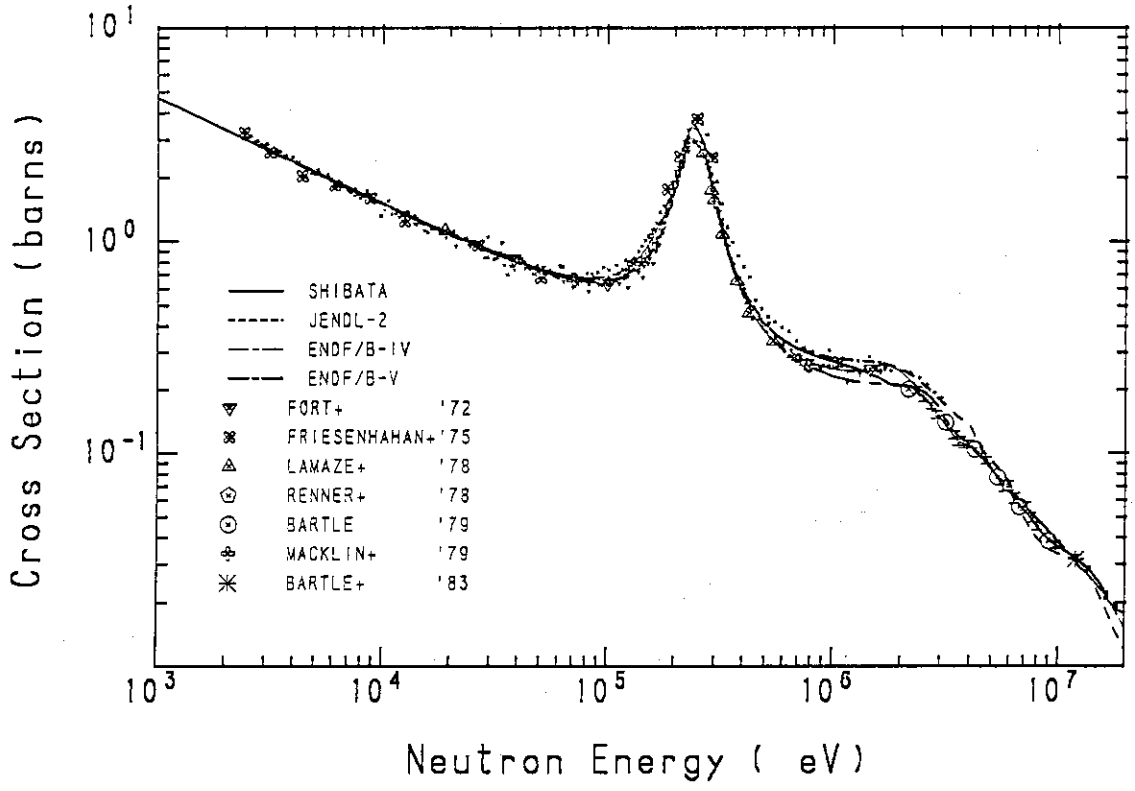

Fig. 13 The $^{6}Li(n,t)\alpha$ Reaction Cross Section

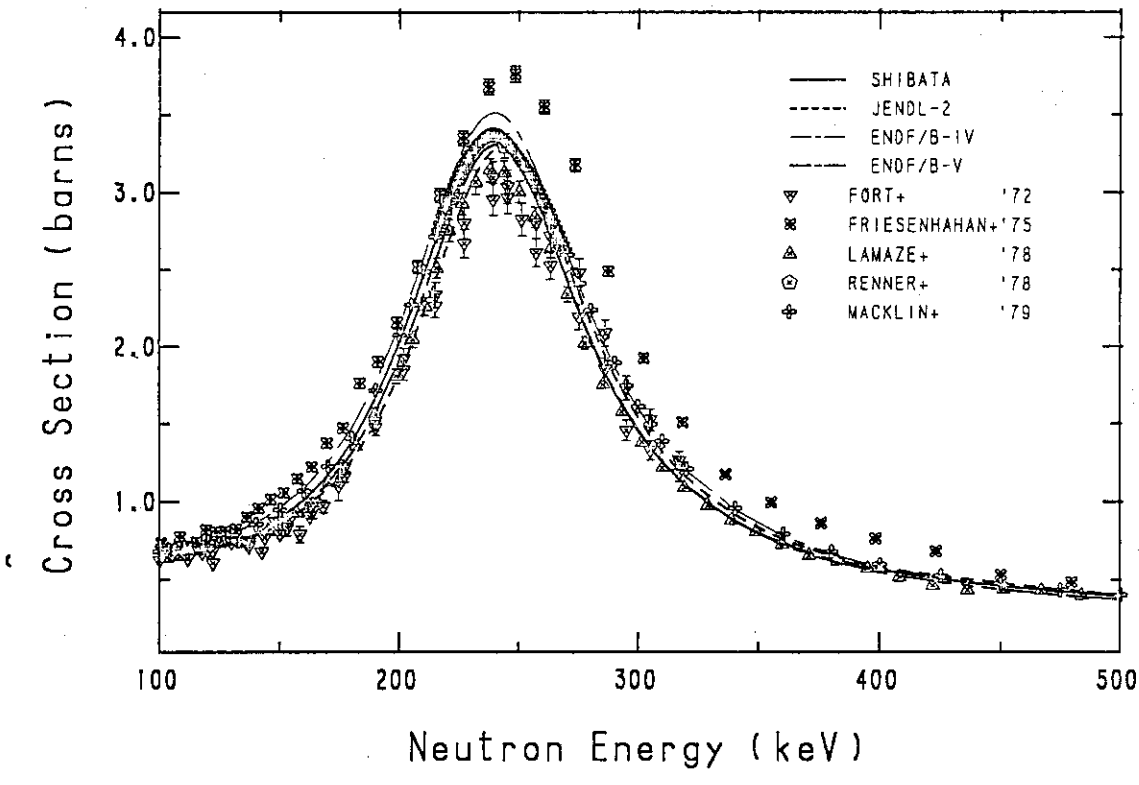

Fig. 14 The $^{6}Li(n,t)\alpha$ Reaction Cross Section (100 ～ 500 keV)

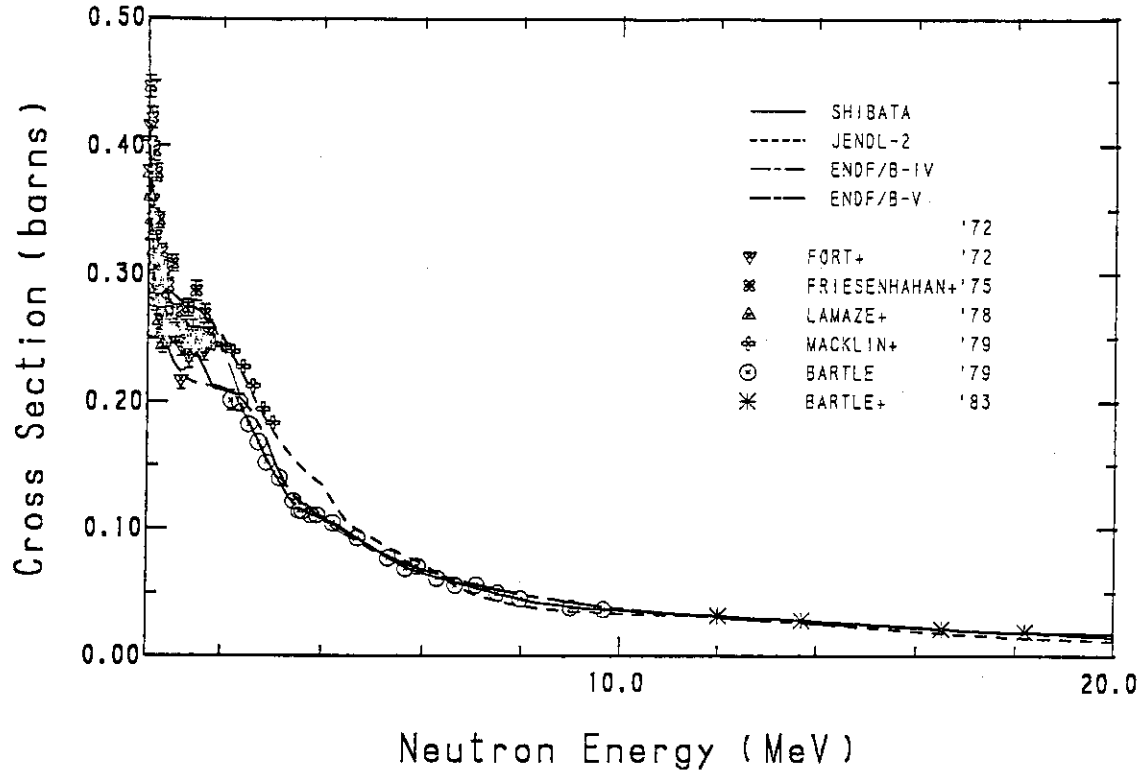

Fig. 15 The $^{6}Li(n,t)\alpha$ Reaction Cross Section (500 keV ～ 20 MeV)

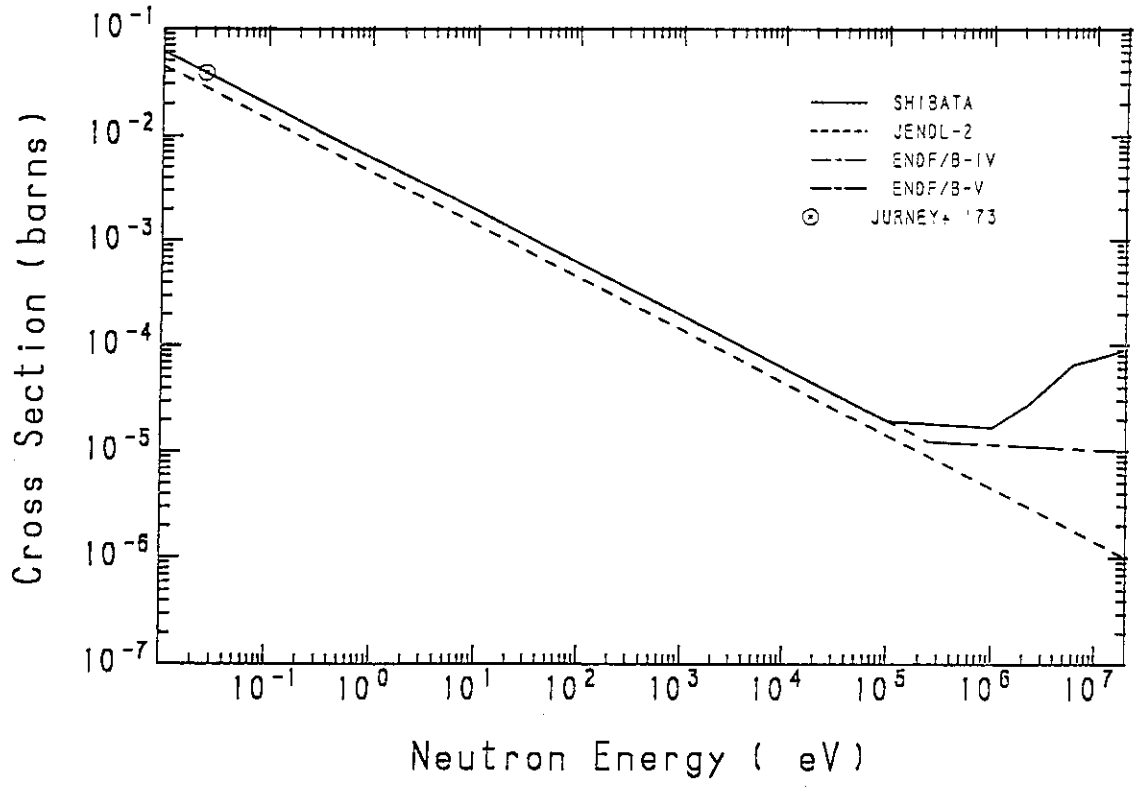

Fig. 16 The $^{6}Li(n,\gamma)$ Reaction Cross Section

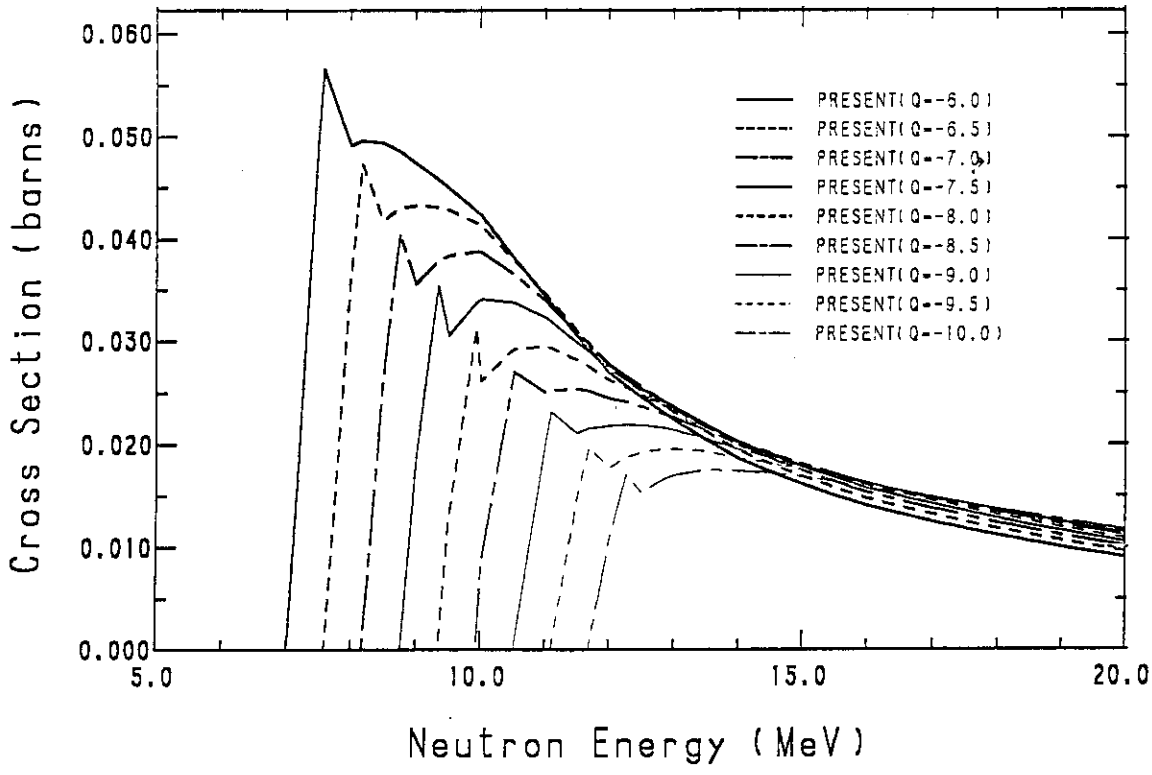

Fig.17 Cross Sections for Pseudo-levels in ^{6}Li

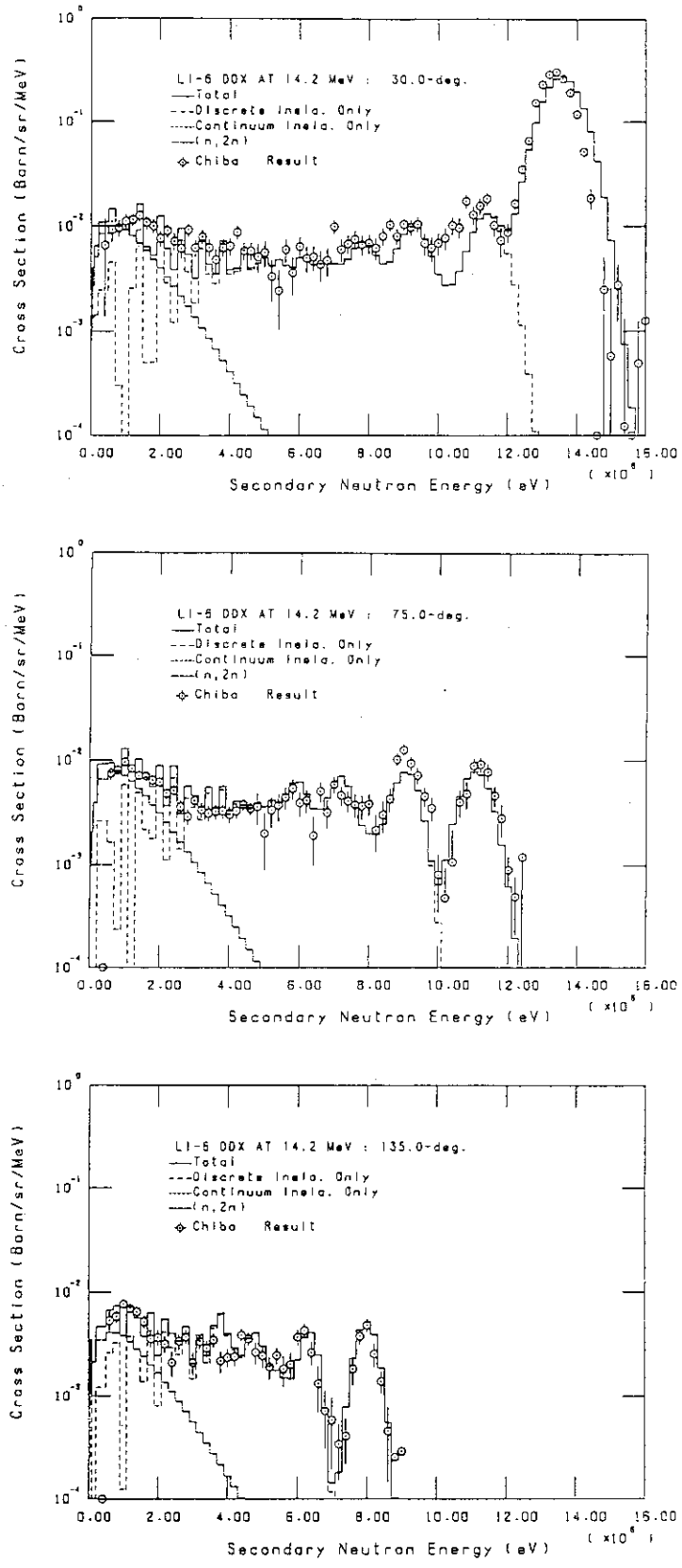

Fig.18 Comparison of the DDX of ^{6}Li produced from the present evaluation (Histograms) with the data measured at Tohoku University at 14.2 MeV

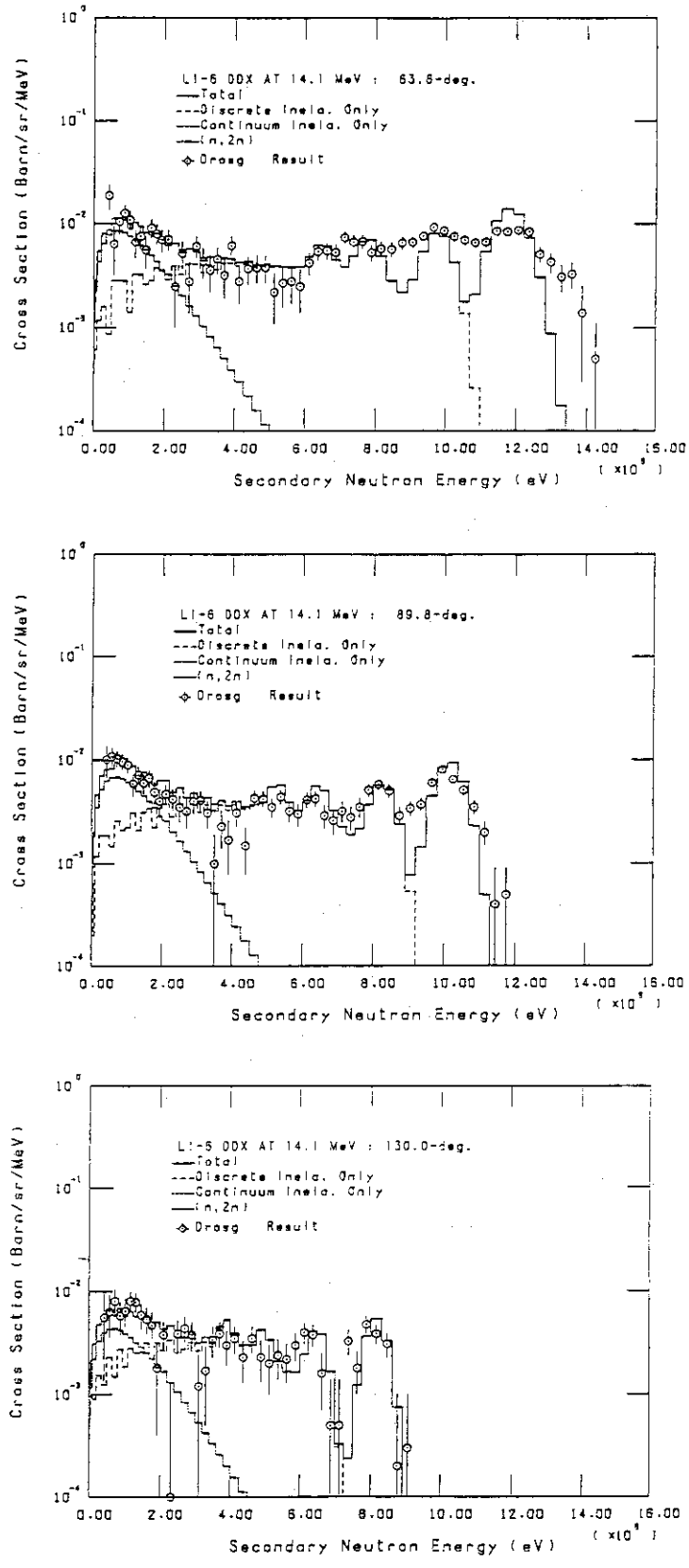

Fig.19 Comparison of the DDX of ^{6}Li produced from the present evaluation with the data measured at LANL at 14.1 MeV

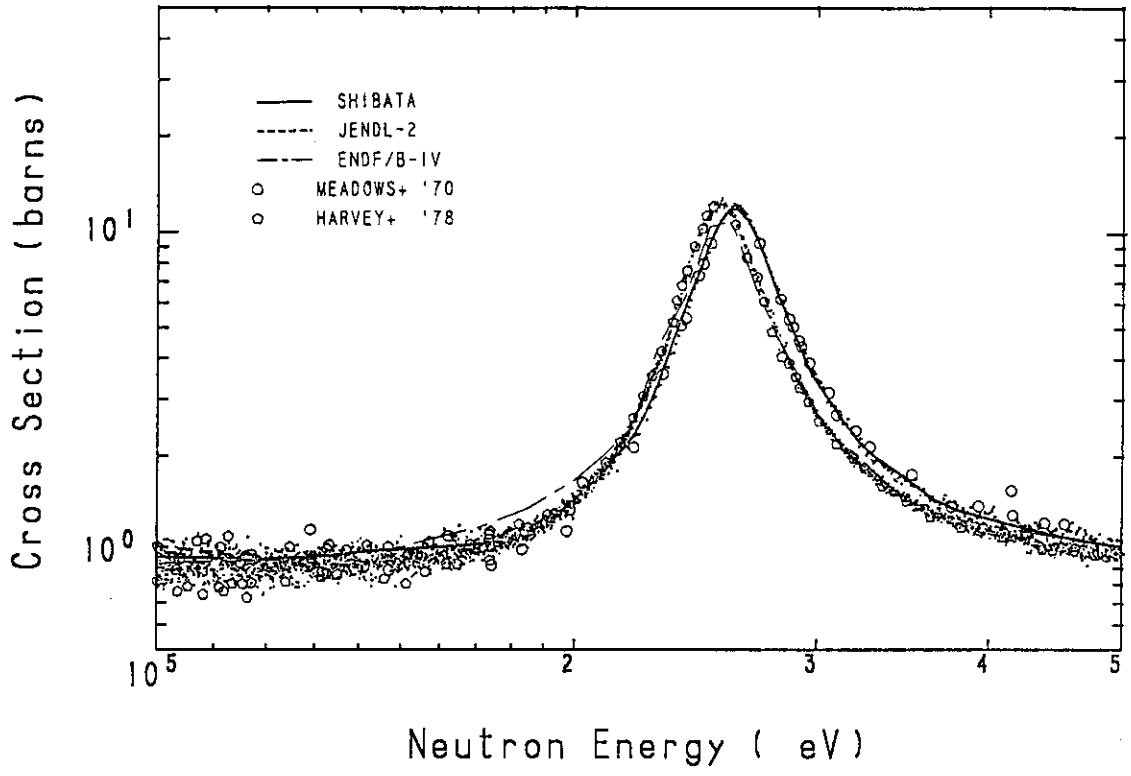

Fig. 20 The Total Cross Section of ^{7}Li (100 ～ 500 keV)

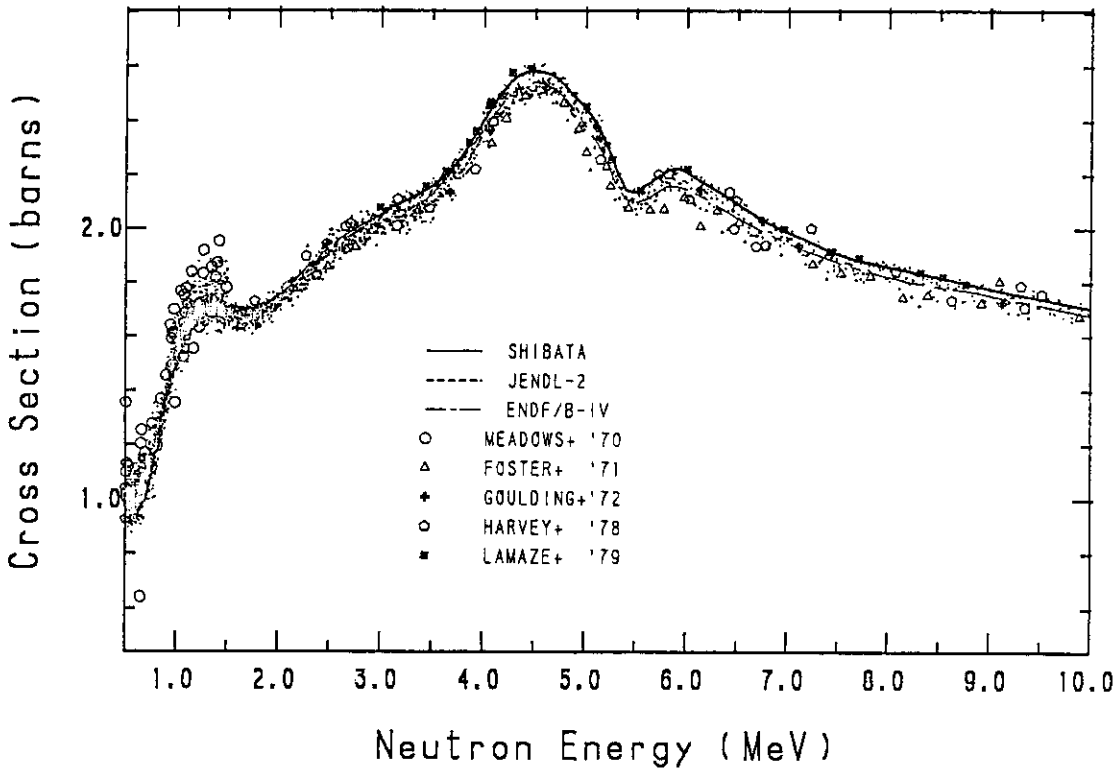

Fig. 21 The Total Cross Section of ^{7}Li (500 keV ～ 10 MeV)

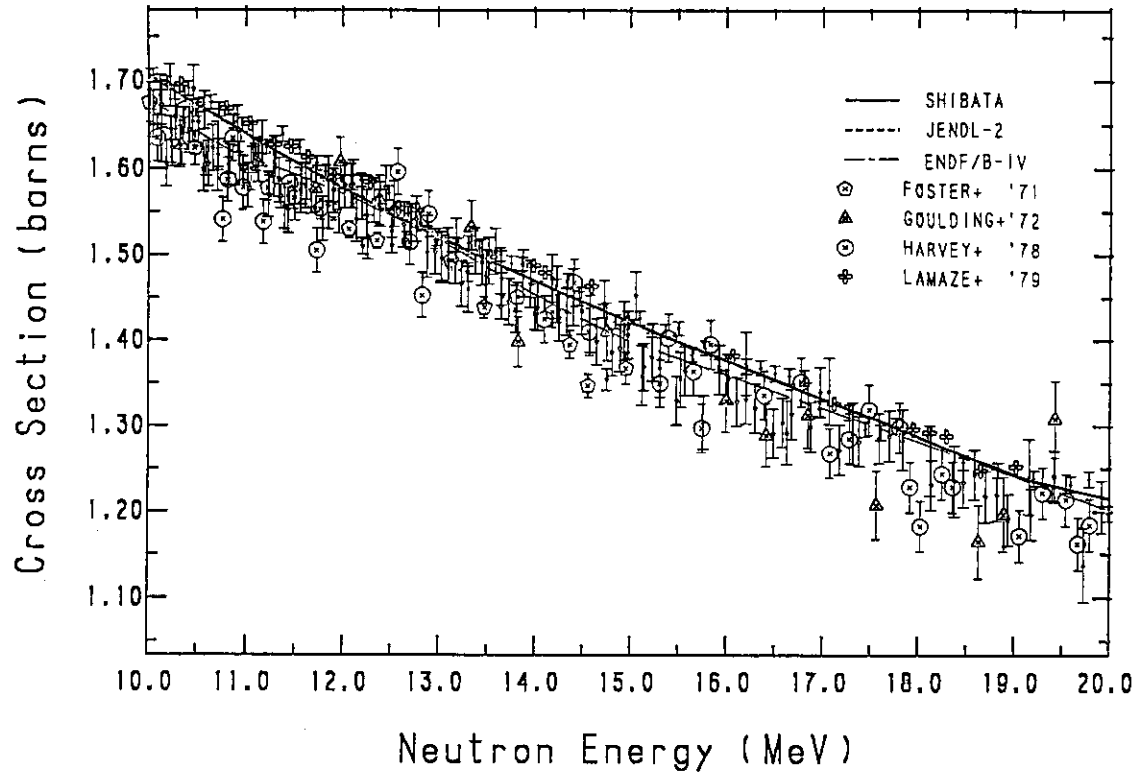

Fig. 22 The Total Cross Section of ^{7}Li (10 ～ 20 MeV)

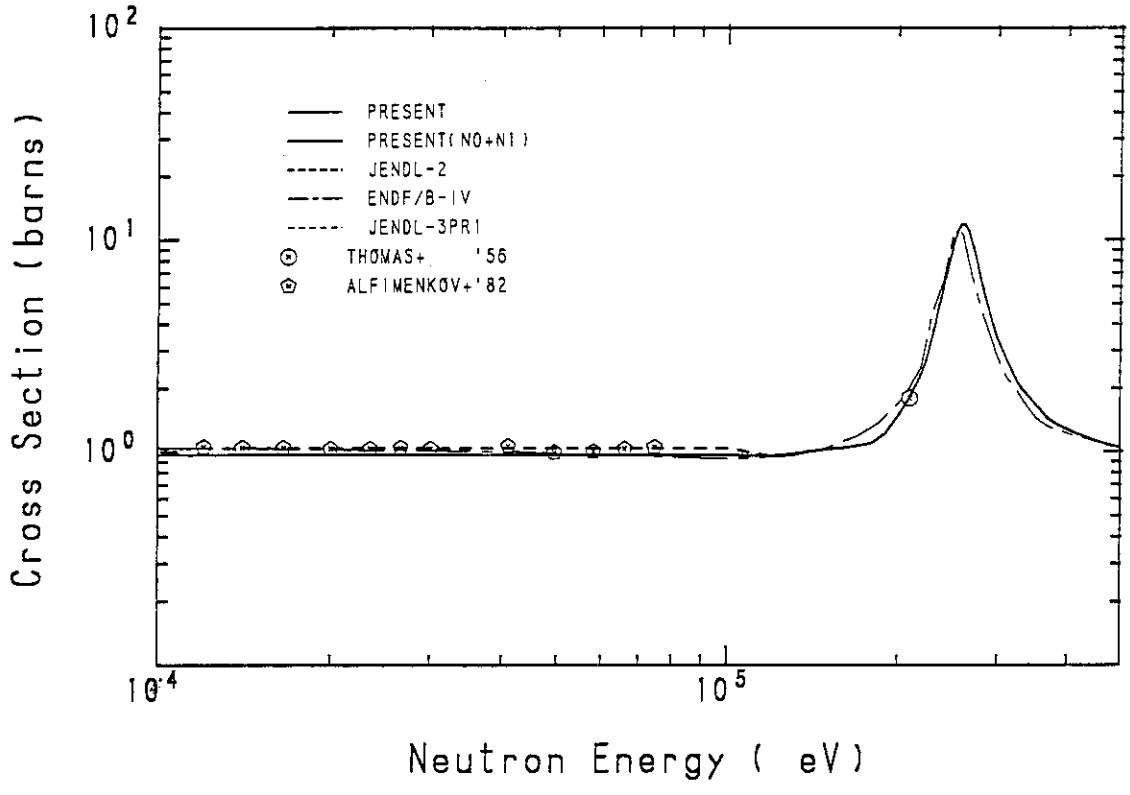

Fig. 23 The Elastic Scattering Cross Section of ^{7}Li (10 ～ 500 KeV)

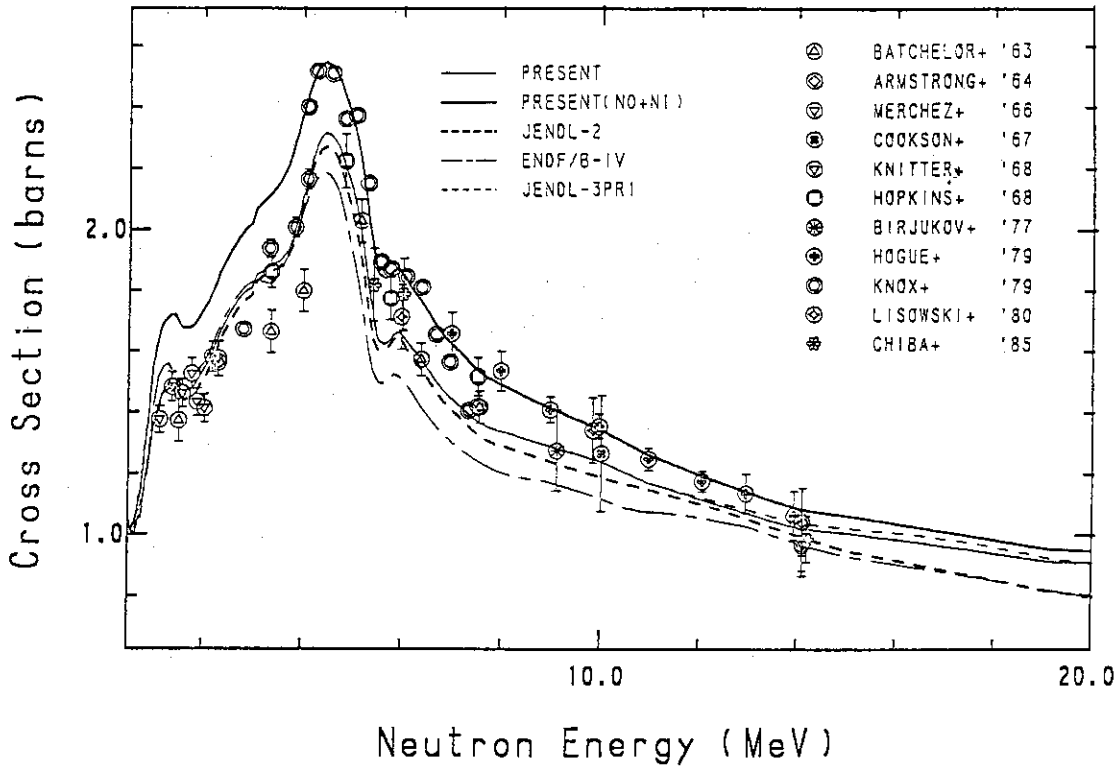

Fig. 24 The Elastic Scattering Cross Section of ^{7}Li(500 keV ～ 20 MeV)

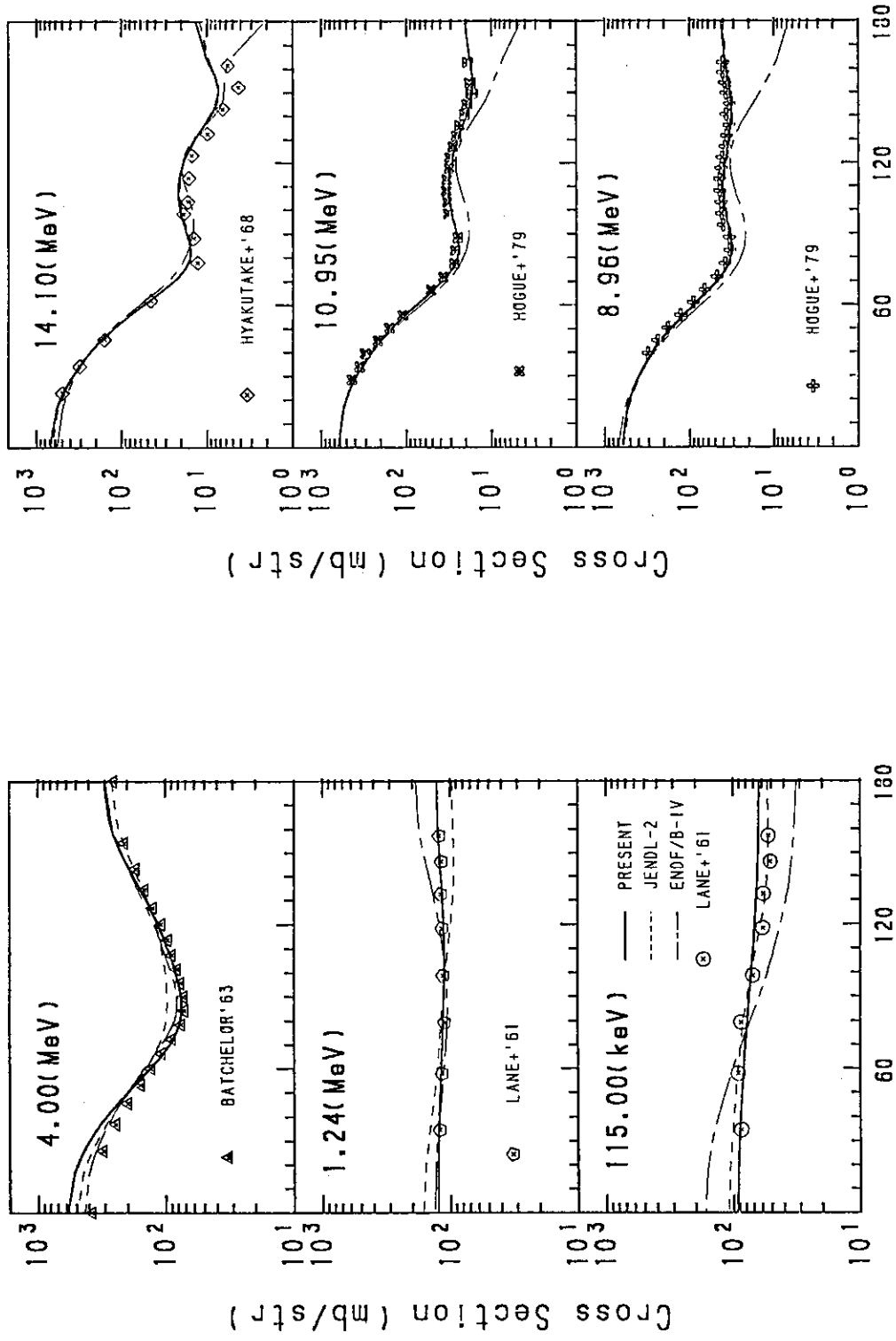

Fig. 25 Angular Distribution of Elastically Scattered Neutrons from ^{7}Li

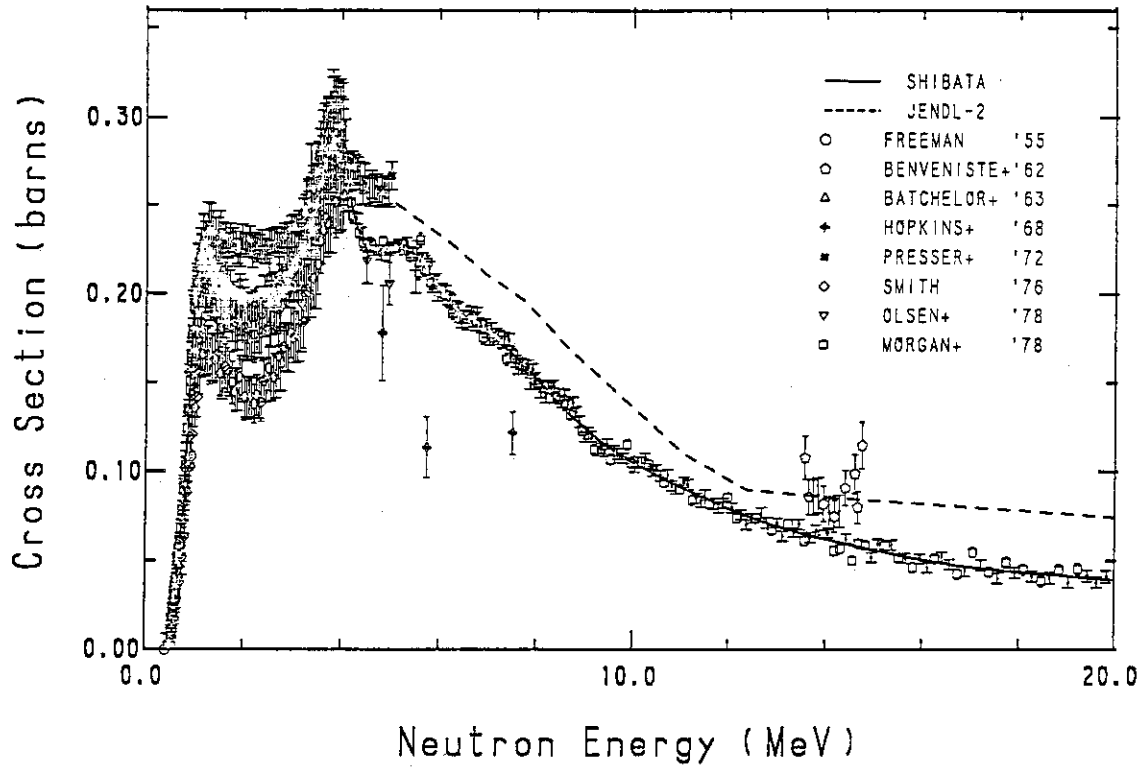

Fig. 26 The $^{7}Li(n,n')^{7}Li^{*}$(0.478 MeV) Cross Section

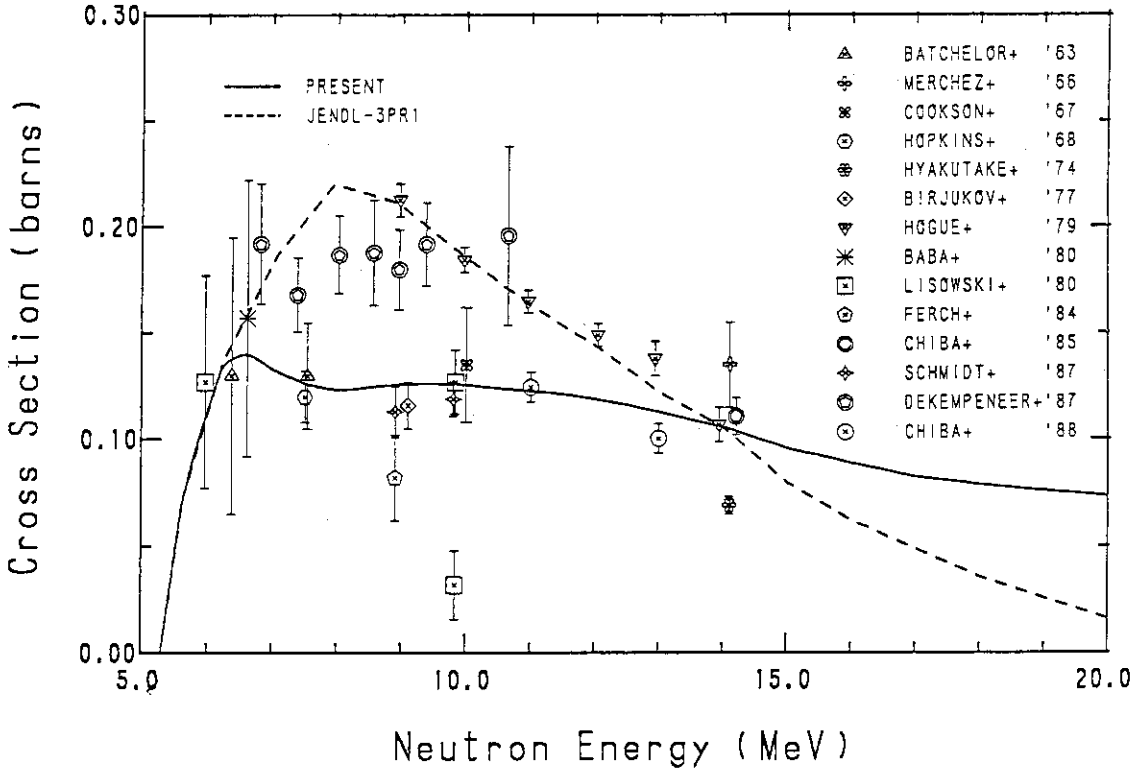

Fig. 27 The $^{7}Li(n,n')^{7}Li^{*}$(4.63 MeV) Cross Section

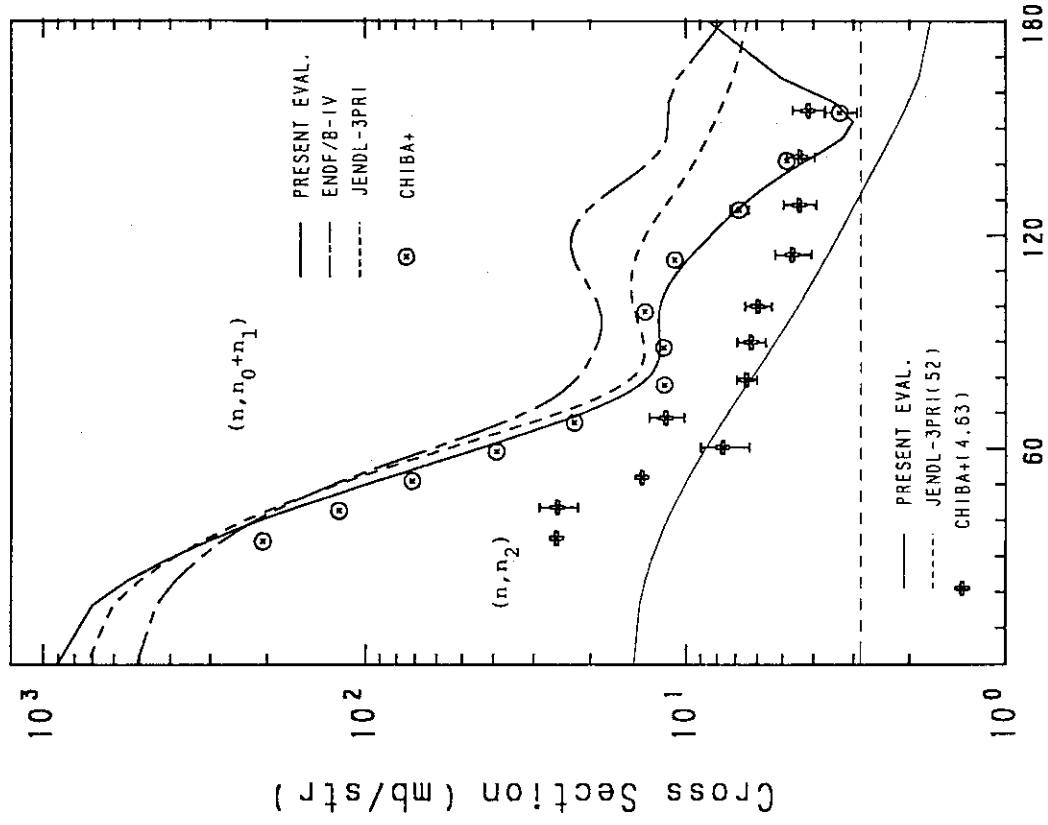

Fig.29 The Angular Distributions of Elasticaly and Inelastically Scatterered Neutrons from ^{7}Li at 18.0 MeV

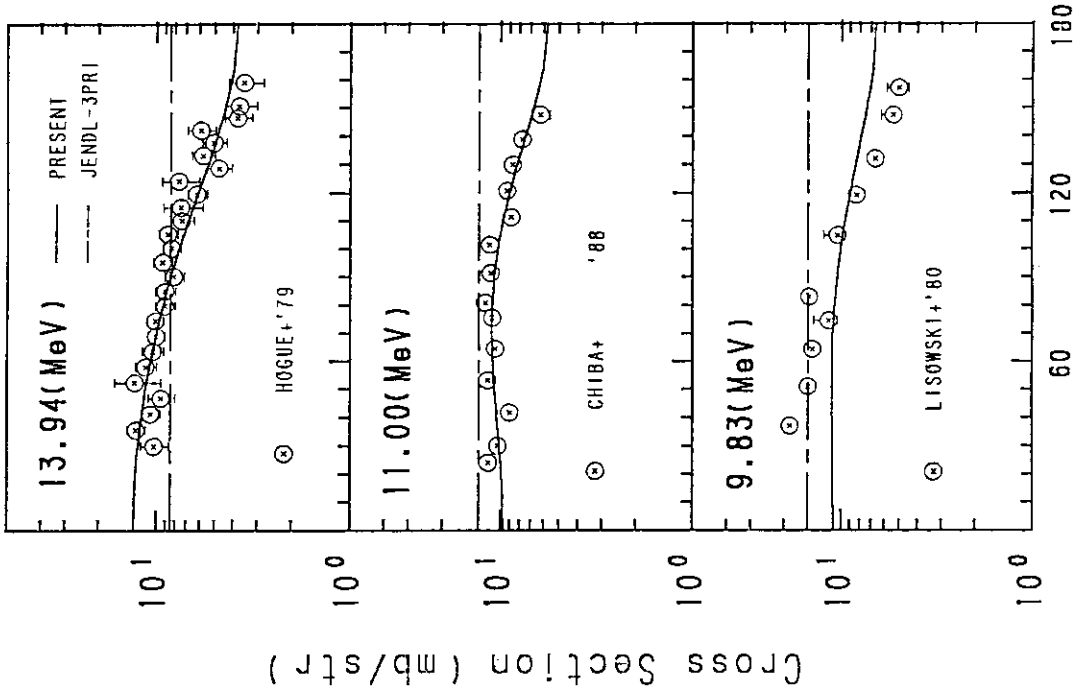

Fig. 28 The Angular Distribution of Inelastically Scattered Neutrons from the 4.63 MeV level in ^{7}Li

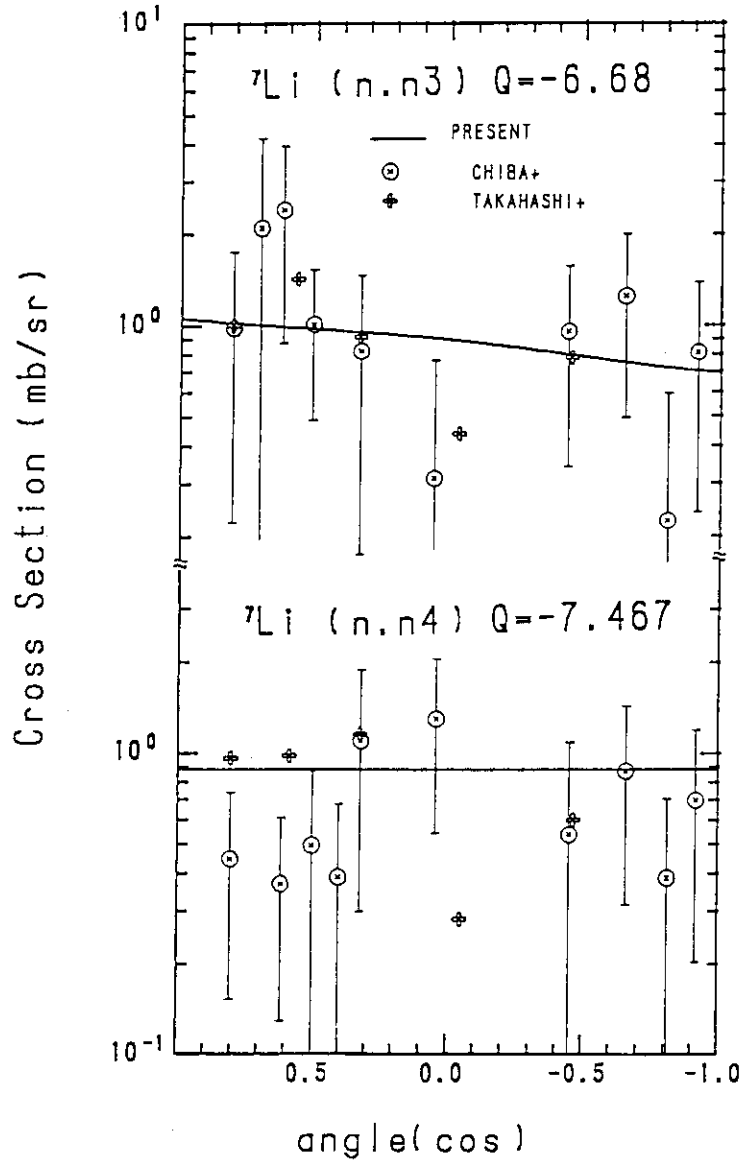

Fig.30 The Angular Distributions of Inelastically Scattered Neutrons from the 6.68 and 7.467-MeV Levels in ^{7}Li

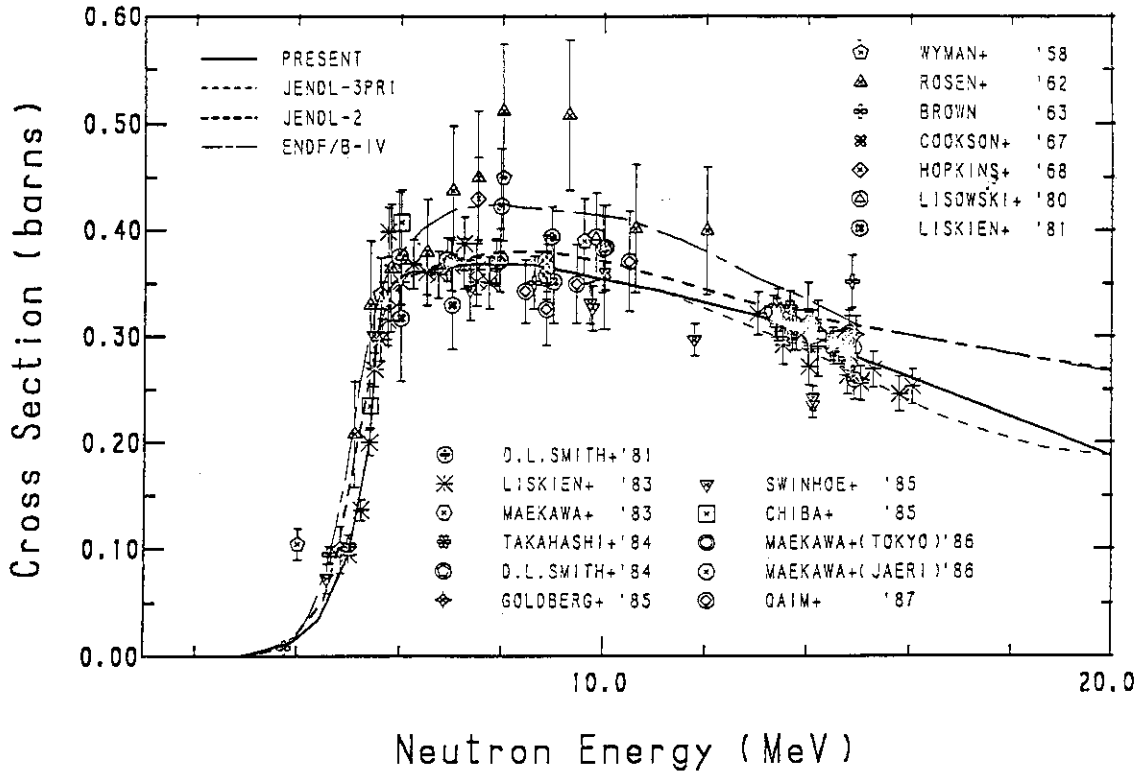

Fig.31 The $^{7}Li(n,n't)\alpha$ Reaction Cross Section

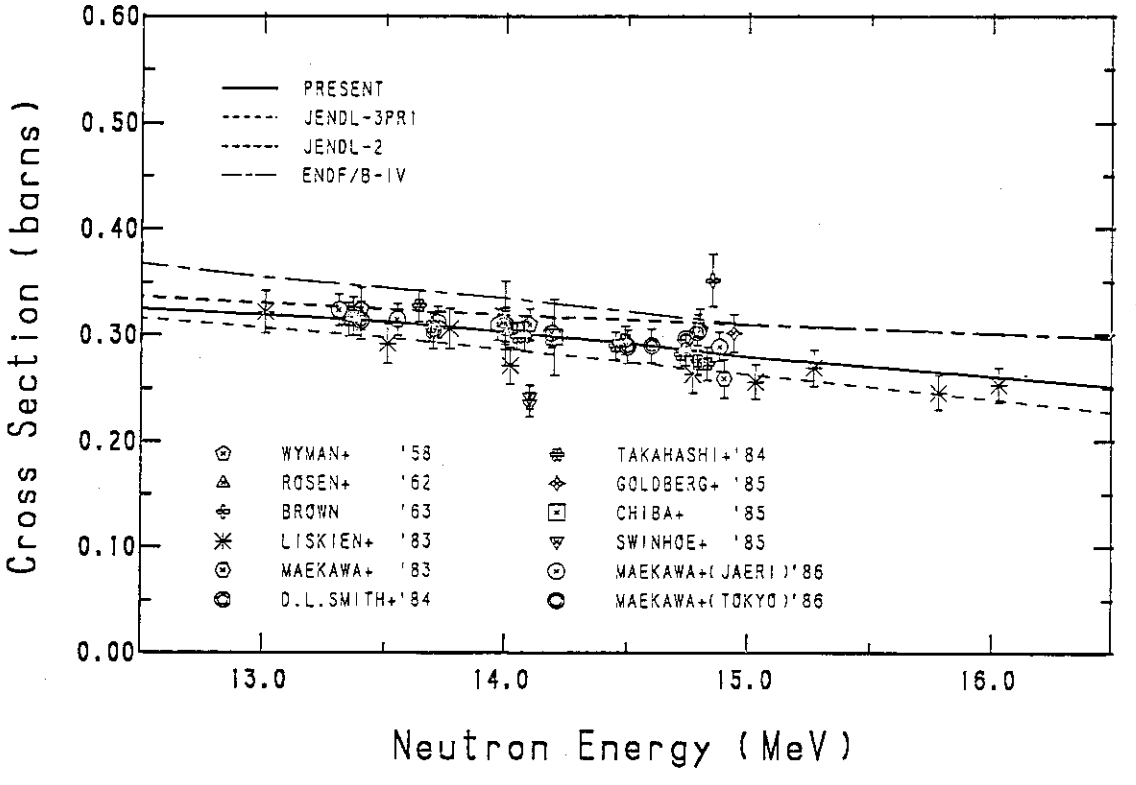

Fig.32 The $^{7}Li(n,n't)\alpha$ Reaction Cross Section (12 ～ 17 MeV)

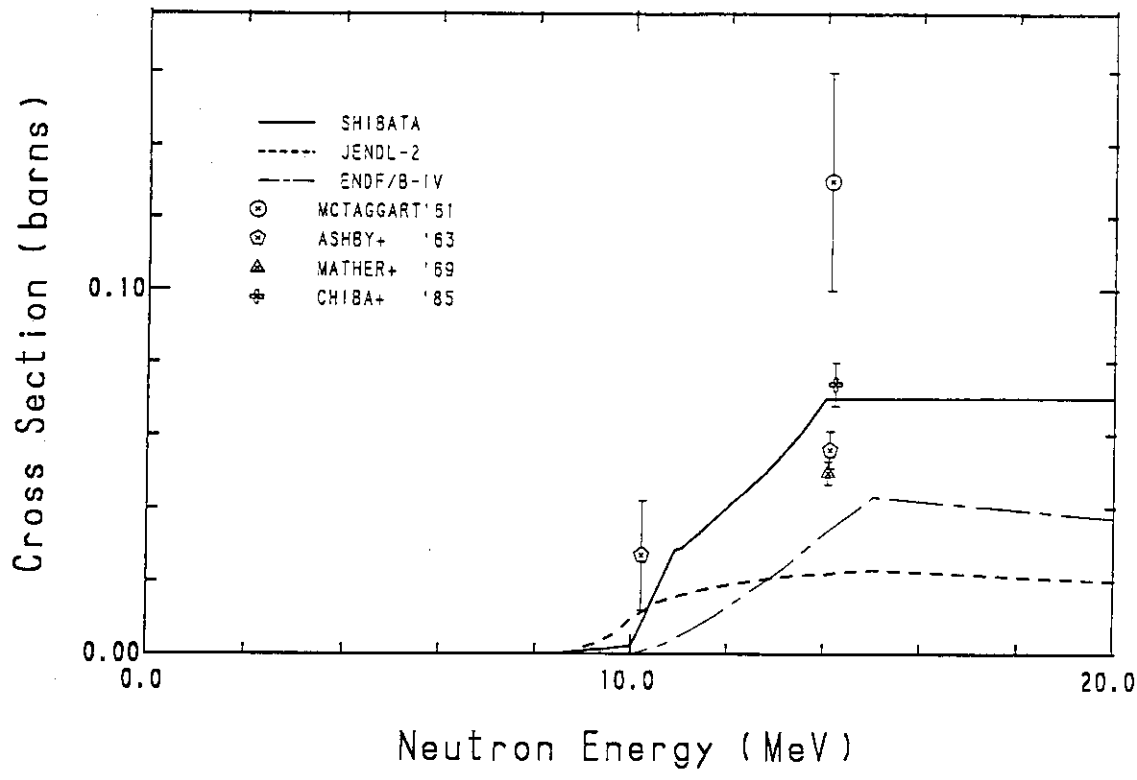

Fig.33 The $^{7}Li(n,2n)$ Reaction Cross Section

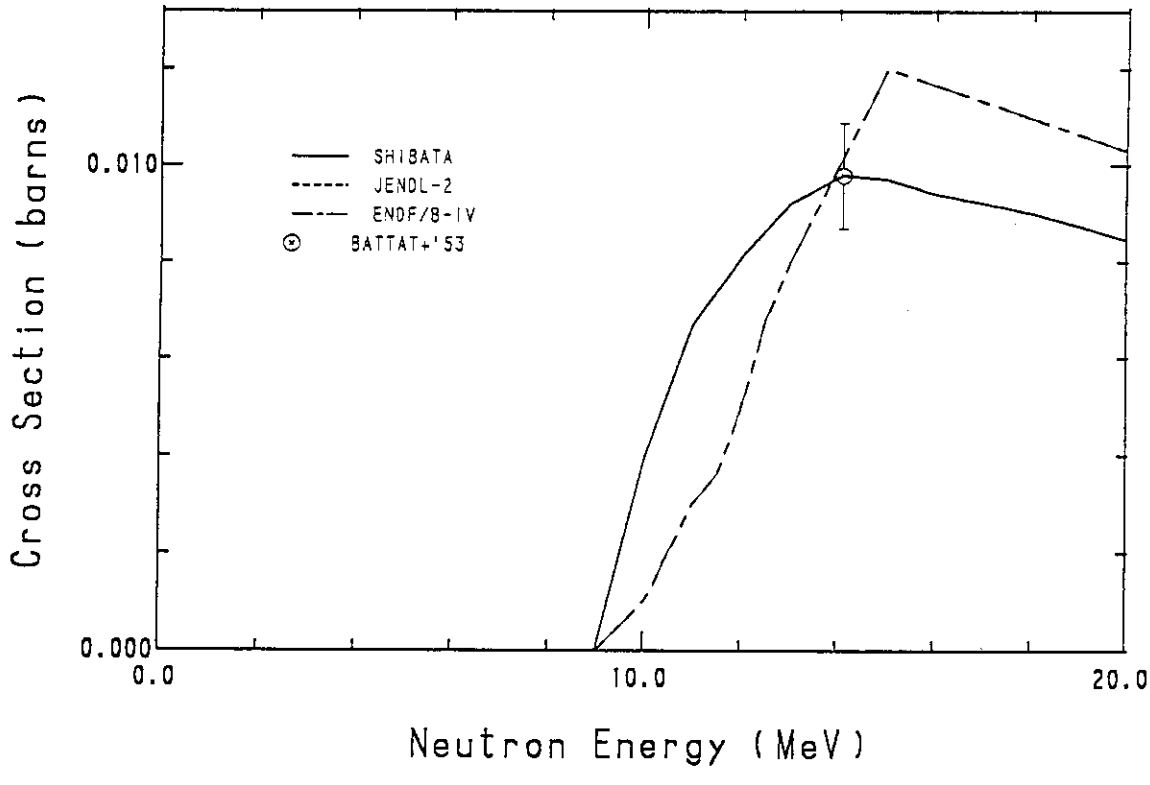

Fig.34 The $^{7}Li(n,d)$ Reaction Cross Section

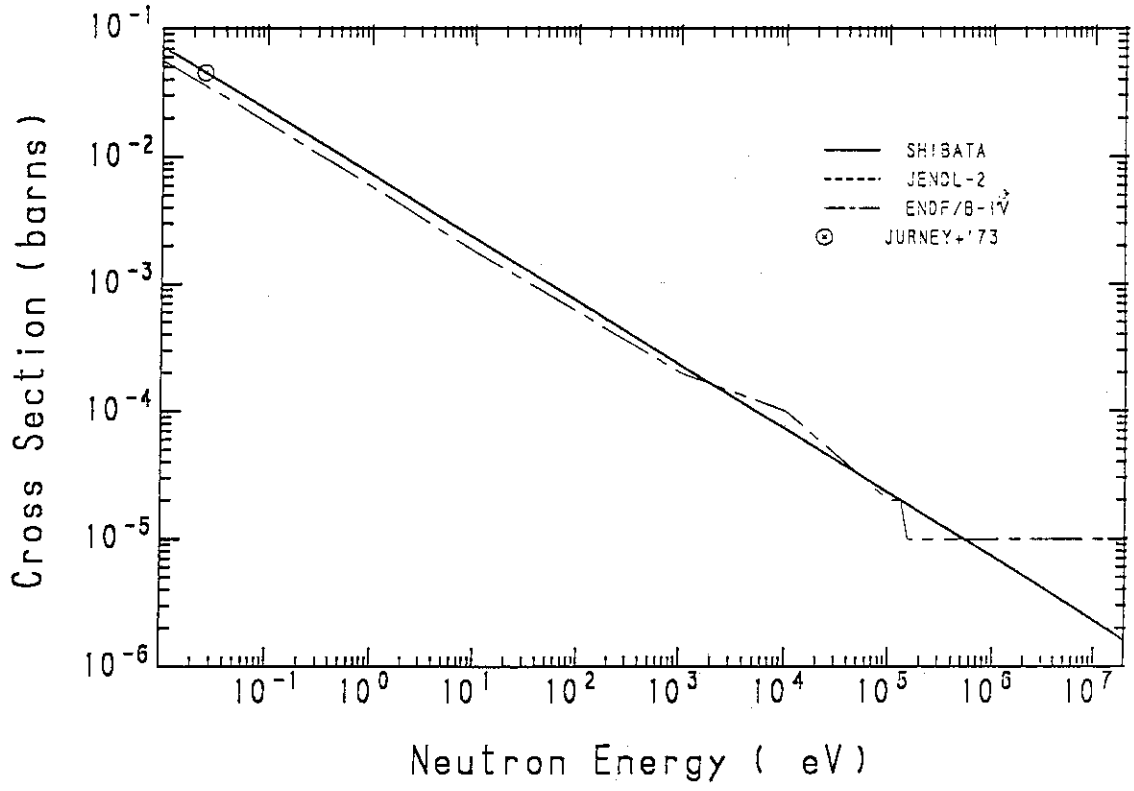

Fig.35 The $^{7}Li(n,\gamma)$ Reaction Cross Section

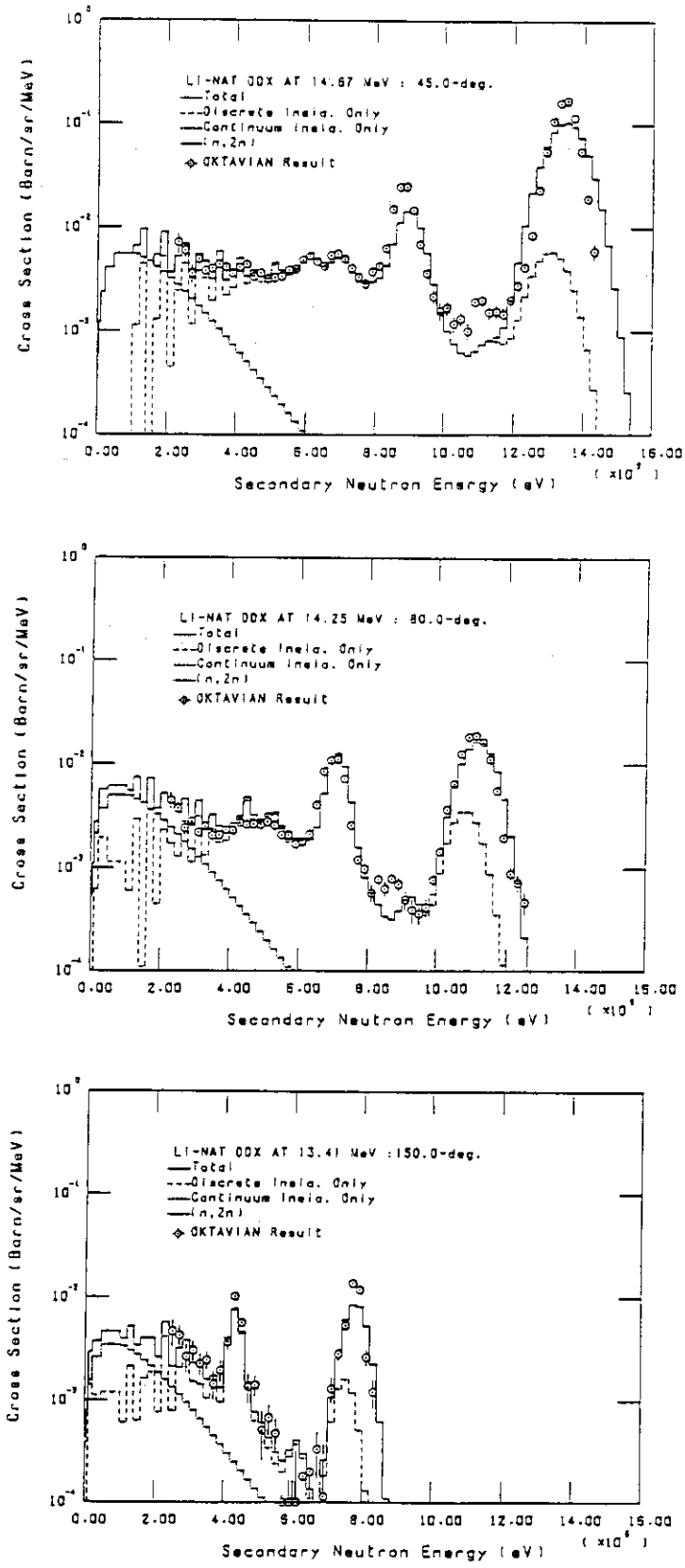

Fig.36 Comparison of the DDX of Natural Lithium produced from the present evaluation (Histogram) with the data measured at Osaka University around 14 MeV

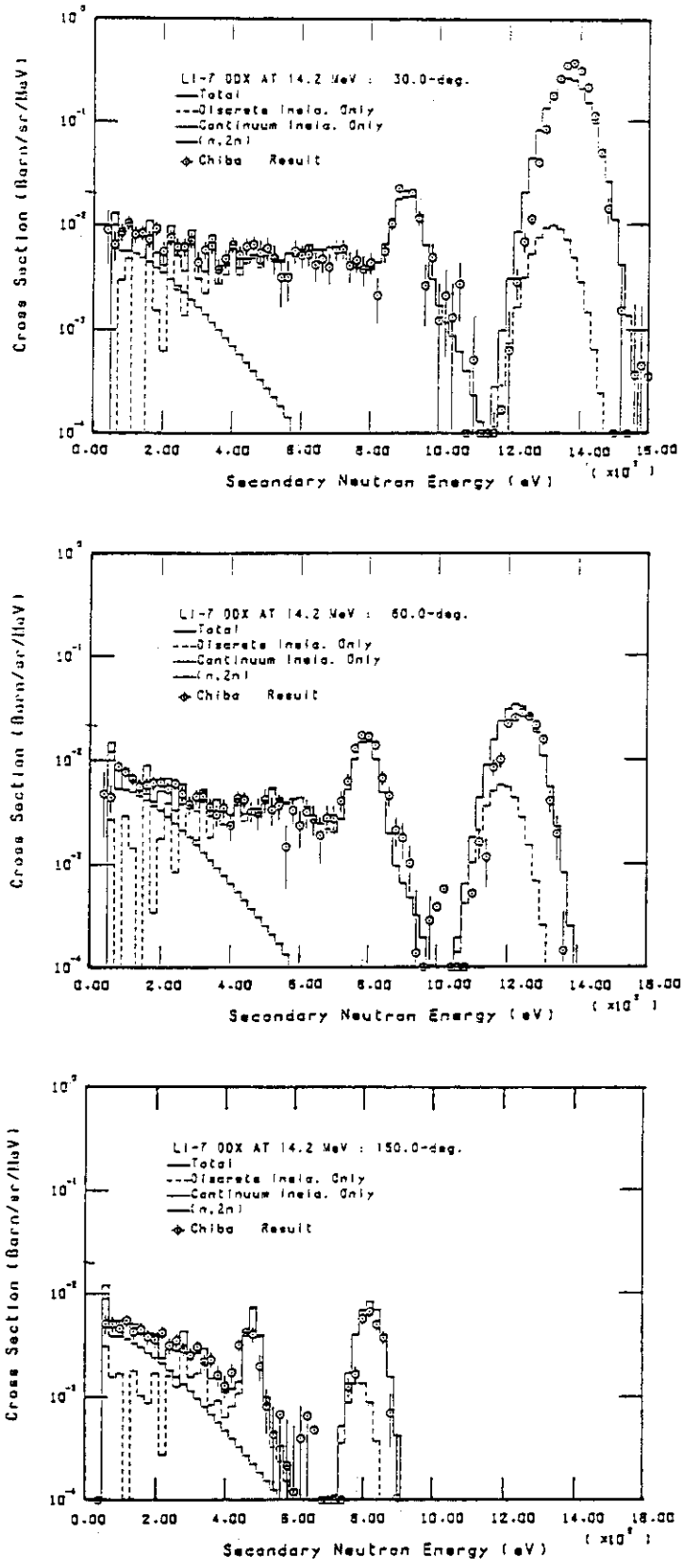

Fig.37 Comparison of the DDX of ^{7}Li produced from the present evaluation with the data measured at Tohoku University at 14.2 MeV

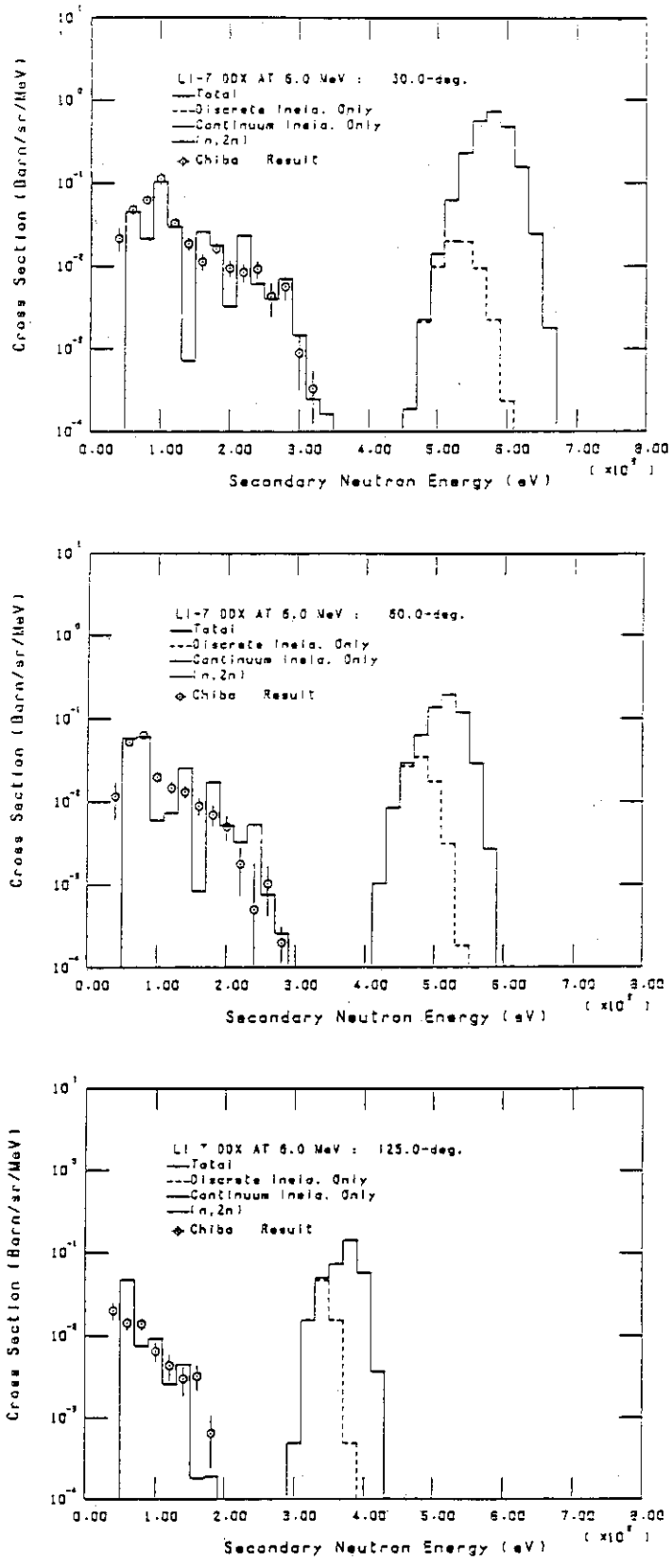

Fig.38 Comparison of the DDX of ^{7}Li produced from the present evaluation with the data measured at Tohoku University at 6.0 MeV